Analysis of the added value of remote sensing soil moisture products for near-future inundation risk assessment in North Brabant, the Netherlands

by

Jeroen Muelders

Universiteit Utrecht

Waterschap Brabantse Delta

Analysis of the added value of remote sensing soil moisture products for near-future inundation risk assessment in North Brabant, the Netherlands

by

Jeroen Muelders

to obtain the degree of Master of Science
finalizing the study Water Science and Management at Utrecht University
to be presented on Thursday September 10, 2020 at 11:00.

Student number:	4265491	
ECTS:	30	
Research duration:	March 2020 – September 2020	
Internship company:	Waterschap Brabantse Delta	
Thesis committee:	Prof. Dr. S.M. de Jong	Utrecht University, supervisor
	Dr. E.A. Addink	Utrecht University, second evaluator
	T. Deurloo MSc	Waterschap Brabantse Delta, supervisor

An electronic version of this thesis is available at https://studenttheses.library.uu.nl/.

Universiteit Utrecht

Waterschap Brabantse Delta

Preface

Dear reader,

This thesis is the result of six months of research as part of the final stage of my master study Water Science and Management at Utrecht University. Regularly this research takes place in the form of an internship. In my case I was granted this opportunity by one of the Dutch regional water authorities, Waterschap Brabantse Delta, situated in Breda. Unfortunately I only had the opportunity to visit and work at the office for two days, after which the events of the global COVID-19 pandemic unfolded. The office became unavailable and working from home became the standard. Regardless, I would like to gratefully thank Waterschap Brabantse Delta for offering me the internship position.

The research would not have been possible without all data providers: HydroLogic for radar precipitation data, the OWASIS soil moisture product, groundwater, and discharge data. VanderSat for their soil moisture product. KNMI for evapotranspiration data. Waterschap Aa en Maas for in-situ soil moisture data and land-use data. Waterschap Brabantse Delta for in-situ soil moisture data.

I thank my supervisors, prof. dr. S. de Jong (Utrecht University) and T. Deurloo MSc (Waterschap Brabantse Delta) for guiding me during the research and sharing their knowledge and experience to improve the research. I thank Dr. Ir. K. Vink (Waterschap Brabantse Delta), E. Zwier (Waterschap Aa en Maas) and F. Bolt (Waterschap Aa en Maas) as well, for providing help and sharing their knowledge and experience to guide the research. I thank ir. G.M. van den Brink (HydroLogic) for providing information on the OWASIS product and its validation. I thank my befriended student T. Roos MSc and my friend C.Q. de Valk BSc for their help with scripting in R and Python. Finally, I thank Dr. E.A. Addink for being the second evaluator of my thesis.

Jeroen Muelders
Gorinchem, September 2020

Summary

Information products that are based on remote sensing data are increasingly being used for operational and strategic water management in the Netherlands. The Dutch regional water authority Brabantse Delta (*Waterschap Brabantse Delta*) is interested in using data products that map the current state of soil moisture content based on remote sensing data. This study aimed to list the currently available soil moisture products for the Netherlands and make analyses on the reliability and the accuracy of those products for the study area in Noord-Brabant. Furthermore, it was analyzed what the relationships was between the amount of precipitation, soil moisture content, groundwater levels, and discharges, in order to find the most important factor in inundation risk assessment. The hypothesis was that such information products could possibly improve decision support systems for inundation risk assessment. In order to incorporate remote sensing soil moisture products in operational water management, there should be a clear understanding of how representative those products are. Two soil moisture data products have been analyzed in detail, the *OWASIS* product by *HydroLogic* and *VanderSat soil moisture* (by *VanderSat*), at 250m and 100m resolution per cell, respectively. In the reliability analyses, the products were statistically compared to in-situ measurements at 15-18 sites and at depths varying between 5 and 20 cm below surface level. This was done at various spatial scales of the data product: one cell, 3x3 cells and at the scale of the full Raam catchment. OWASIS showed a very weak Pearson correlation of R=0.29 (*single cell site average*), 0.31 (*3x3-grid of cells*), 0.18 (*catchment scale*). It was found that OWASIS models the soil moisture in the rootzone rather than the full unsaturated zone. OWASIS does not report the (dynamic) depth of the rootzone, rendering the data unusable for inundation risk assessment. The VanderSat product showed a moderate to strong correlation with in-situ measurements: R=0.66 (*single cell site average*) and R=0.82 (*catchment scale*). The mean absolute error for VanderSat compared to in-situ measurements was 0.068 [m^3/m^3] (*single cell*) and 0.031 [m^3/m^3] (*catchment scale*). The spatial and temporal variability in soil moisture content among individual sites was much higher in-situ compared to the VanderSat product, the VanderSat product is particularly smooth in spatial distribution compared to the much more dynamic observations at the in-situ sites. The basic rainfall-runoff analysis showed a clear gradient from low to high discharge when transitioning from (relatively) deep to medium to shallow groundwater levels; while for the soil moisture content the transition from medium to wet conditions showed more of a mixed nature, i.e. some wet conditions showed medium discharges and some medium soil moisture conditions showed high discharge. This indicates that for precipitation events in the study area the discharge is generally stronger correlated to groundwater depth than to soil moisture content. Though, in more rare cases soil moisture conditions were more important than groundwater levels, as was shown by a small number of events in which the groundwater level was relatively close to the surface, while discharge remained low due to dry soil moisture conditions. The study concludes that the investigated soil moisture products that are based on remote sensing data are currently an unfeasible option to improve the assessment of near-future inundation risk for the province of Noord-Brabant, the Netherlands, because the available products are either unreliable or too smooth to provide accurate soil moisture content estimates at cell scale (100 - 250 m). The VanderSat product showed some potential to be used at catchment scale (approx. 100 km^2), but it depends on the application whether this is sufficient for operational use. Due to the fact that soil moisture conditions were generally shown to be less important in (high) runoff generation than the level of the groundwater, it would be advisable to focus on other options than remote sensing soil moisture content for inundation risk assessment.

Samenvatting

Informatieproducten die zijn gebaseerd op satellietgegevens worden in toenemende mate gebruikt voor operationeel en strategisch waterbeheer in Nederland. Waterschap Brabantse Delta is geïnteresseerd in het gebruik van dataproducten die op basis van satellietgegevens de actuele stand van het bodemvocht in kaart brengen. Het onderzoek had tot doel om de momenteel beschikbare bodemvochtproducten voor Nederland in kaart te brengen en analyses te doen op de betrouwbaarheid en nauwkeurigheid van die producten voor het studiegebied in Noord-Brabant. Verder is geanalyseerd wat de relaties zijn tussen hoeveelheid neerslag, bodemvochtgehalte, grondwaterstanden en afvoeren, om de belangrijkste factor bij de risicobeoordeling van inundatie (overstroming) te vinden. De hypothese was dat dergelijke informatieproducten mogelijk de besluitvormingsondersteunende systemen (BOS) voor de beoordeling van overstromingsrisico's zouden kunnen verbeteren. Om bodemvochtproducten o.b.v. satellietgegevens volledig te kunnen integreren in het operationele waterbeheer, moet er duidelijk inzicht zijn in hoe representatief die producten zijn. Twee dataproducten voor bodemvocht zijn in detail geanalyseerd, het OWASIS-product van HydroLogic en VanderSat soil moisture (van VanderSat), met respectievelijk resoluties van 250m en 100m per cel. In de betrouwbaarheidsanalyses werden de producten statistisch vergeleken met in-situ metingen op 15-18 locaties en op dieptes variërend tussen 5 en 20 cm onder maaiveld. Dit gebeurde op verschillende ruimtelijke schalen van het dataproduct: één cel, 3x3 cellen en op de schaal van het volledige Raam-stroomgebied. OWASIS vertoonde een zwakke Pearson-correlatie van R = 0,29 (gemiddelde van één cel op meerdere locaties), 0,31 (3x3-raster van cellen, gemiddeld over de locaties), 0,18 (schaal van het stroomgebied). Het bleek dat OWASIS het bodemvocht in de wortelzone modelleert in plaats van de volledige onverzadigde zone. OWASIS rapporteert echter niet de (dynamische) diepte van de wortelzone, waardoor de gegevens onbruikbaar worden voor inundatierisicobeoordeling. Het VanderSat-product vertoonde een matige tot sterke correlatie met in-situ metingen: R = 0,66 (gemiddelde van één cel op meerdere locaties) en R = 0,82 (schaal van het stroomgebied). De gemiddelde absolute fout (*mean absolute error*) voor VanderSat vergeleken met in-situ metingen was 0,068 [m³/m³] (één cel) en 0,031 [m³/m³] (stroomgebiedsschaal). De ruimtelijke en temporele variabiliteit in bodemvochtgehalte tussen individuele locaties was in-situ veel hoger in vergelijking met het VanderSat-product, het VanderSat-product is relatief homogeen in de ruimtelijke variabiliteit. De basale neerslag-afvoeranalyse liet een duidelijke gradiënt zien van lage naar hoge afvoer bij de overgang van (relatief) diepe naar gemiddelde naar ondiepe grondwaterstanden; terwijl voor het bodemvochtgehalte de overgang van gemiddelde naar natte condities een meer gemengd karakter vertoonde, dat wil zeggen dat sommige natte condities gemiddelde afvoeren opleverden en sommige gemiddelde bodemvocht condities een hoge afvoer. Dit geeft aan dat voor neerslaggebeurtenissen in het studiegebied de grondwaterdiepte in het algemeen meer invloed heeft op de afvoerproductie dan het bodemvochtgehalte. In zeldzamere gevallen waren de bodemvochtigheid echter belangrijker dan de grondwaterstand, zoals bleek uit een klein aantal gebeurtenissen waarbij de grondwaterstand relatief dicht bij het oppervlak lag, terwijl de afvoer laag bleef door het lage bodemvochtgehalte. De studie concludeert dat de onderzochte bodemvochtproducten die zijn gebaseerd op satellietgegevens momenteel een onwenselijke optie zijn om de beoordeling van het inundatierisico te verbeteren voor de provincie Noord-Brabant. Dit omdat de beschikbare producten ofwel onbetrouwbaar ofwel te homogeen zijn om nauwkeurige schattingen van het bodemvochtgehalte op cel-schaal te geven (100 - 250 m). Het VanderSat-product vertoonde enig potentieel voor toepassing op stroomgebiedsschaal (ca. 100 km²), maar het hangt van de toepassing af of dit voldoende is voor operationeel gebruik. Omdat bovendien werd aangetoond dat in het algemeen bodemvochtgehalte minder belangrijk is bij het genereren van (hoge) afvoeren dan het niveau van het grondwater, is het raadzaam om voor inundatierisico's te focussen op andere opties dan satelliet-verkregen bodemvochtgehalte.

Contents

List of abbreviations

DSS	Decision support system
GW	Groundwater
LHM	Landelijk Hydrologisch Model (*Dutch National Hydrologic Model*)
RS	Remote Sensing
SM	Soil Moisture
WSAM	Waterschap Aa en Maas
WSBD	Waterschap Brabantse Delta

1 Introduction

Information products that are based on remote sensing data are increasingly being used for operational and strategic water management in the Netherlands. Well-integrated examples are digital elevation models, land-use mapping, and precipitation forecasting. In recent years, water managing authorities have started experimenting with the use of other remote sensing products such as actual evaporation and soil moisture content. Certain products may also combine individual data sources into a more advanced product through data assimilation techniques. These soil moisture products are, however, not yet fully incorporated in operational water management.

The Dutch regional water authority Brabantse Delta (*Waterschap Brabantse Delta*) is interested in using remote sensing products that map the current state of soil moisture content. Such maps may aid the water authority in managing water levels for the purpose of reducing the impacts of inundations or droughts. Inundations may occur due to heavy precipitation events. However, the state of the unsaturated zone in terms of soil moisture content and the thickness of the unsaturated zone may also play an important role; previously, some heavy precipitation events have caused no damage, while other events of similar intensity and duration do have caused significant inundation damage.

In order to fully incorporate remote sensing soil moisture products in operational water management, there should be a clear understanding of how representative those products are for the actual soil moisture state. Furthermore, there is an interest at the water authority to research whether remote sensing soil moisture data can aid in inundation risk assessment, by improving rainfall-runoff models and decision support systems (DSS) (*beslissingsondersteunende systemen*). The relationships between (remote sensing) soil moisture content, groundwater levels, amount of precipitation, and historic records of discharge may provide useful insights for rainfall-runoff modeling and DSS to mitigate the effects of inundation and droughts.

The current DSS at Brabantse Delta uses weather forecasts and simplified schematizations of the main system. It also uses precipitation data (radar), evaporation (KNMI), and water levels outside the Brabantse Delta system (measured and modeled). The DSS is used to estimate what is to come in the event of extreme discharge, and to support the deployment of various measures that can be taken in the water system. Remote sensing is currently only used in the form of precipitation data (radar), actual evapotranspiration (not used in any operational processes, but sometimes serves as input for rainfall-runoff models), and digital elevation models (AHN). There are currently no direct connections between models and remote sensing products, e.g. remote sensing soil moisture data is not used.

1.2 Previous research

Validation of remotely sensed soil moisture data to in-situ data has been the topic of various studies. Albergel *et al*. (2012) evaluated and compared one analysis from the ECMWF[1] numerical weather prediction system (SM-DAS-2) and two remote sensing soil moisture products, being ASCAT (Advanced Scatterometers) and SMOS (Soil Moisture Ocean Salinity), to in-situ soil moisture data of over 200 stations globally. Correlation with in-situ measurements were deemed "very satisfactory […] with averaged values of 0.70 for SM-DAS-2, 0.53 for ASCAT and 0.54 for SMOS". Wanders *et al.* (2012) determined the uncertainty of satellite soil moisture products over Spain using a deterministic, distributed unsaturated zone model (SWAP). Temporal dynamics were best captured by AMSR-E and ASCAT satellites with averaged correlation coefficients of 0.68 and 0.71, respectively. SMOS showed the capability of capturing long-term trends, however on short timescales the soil moisture signal was not captured as well as by the other sensors, resulting in an averaged correlation coefficient of 0.42. Validation of SMAP (Soil Moisture Active Passive) passive-only satellite data to in-situ data (20 stations) was done for the region of Twente, the Netherlands (Velde *et al*., 2019). The best agreement with their in-situ references led to an unbiased Root-Mean-Squared-Error (uRMSE) of $0.059\,m^3\,m^{-3}$. Once filtered for frozen conditions and antecedent rainfall the uRMSE improved to $0.043\,m^3\,m^{-3}$.

All soil moisture products mentioned in the previous paragraph vary in spatial resolution from 25 to 50 km per pixel, which is often not detailed enough for operational water management on a local to regional catchment scale. To illustrate this, the entire Brabantse Delta area would be covered by only 1 or 2 pixels. More recent satellite sensors such as the Synthetic Aperture Radar (SAR) onboard Sentinel-1 combined with optical data from Sentinel-2 make it possible to retrieve soil moisture at 1000 to 100 m resolution with a RMS error in volumetric moisture of 0.059 $m^3\ m^{-3}$ (Gao *et al.*, 2017). More and more often, methods using computer algorithms and data assimilation are being developed; these combine multiple data sources to improve the (relatively low) spatial resolution of remotely sensed data up to 250 m (OWASIS) (ESA, 2019) and 100 m (VanderSat, n.d.).

1.3 Research aim and questions

The scientific aim of this study was to gain (1) better knowledge on the quality of (remote sensing) soil moisture data products with respect to spatial and temporal variation between those products and in-situ measurements of the soil moisture content, as well as (2) improved knowledge on the impact of soil moisture conditions and groundwater levels on the conversion of precipitation into discharge, to assess near-future risks of inundation in the study area. Apart from the scientific relevance, this aim also has an embedded social relevance because the water authorities are responsible for flood and drought prevention management, mitigating negative effects of inundations and droughts. The research aims to provide insights to possibly improve models and decision support systems, which the water authorities use for operational management strategies. To achieve the aims, the following research question is formulated and divided into three sub-questions:

Can soil moisture products that are based on remote sensing data improve the assessment of near-future inundation risk for the province of Noord-Brabant, the Netherlands?

1. What soil moisture products that are based on remote sensing data are currently available for the Netherlands, what are their spatial and temporal resolutions, and what validation has been done with respect to these products?
2. How reliable and accurate are the available soil moisture products for the study area?
3. What information can the relation between precipitation, soil moisture state, groundwater depth and discharge add to inundation risk assessment?

[1] European Centre for Medium-Range Weather Forecasts

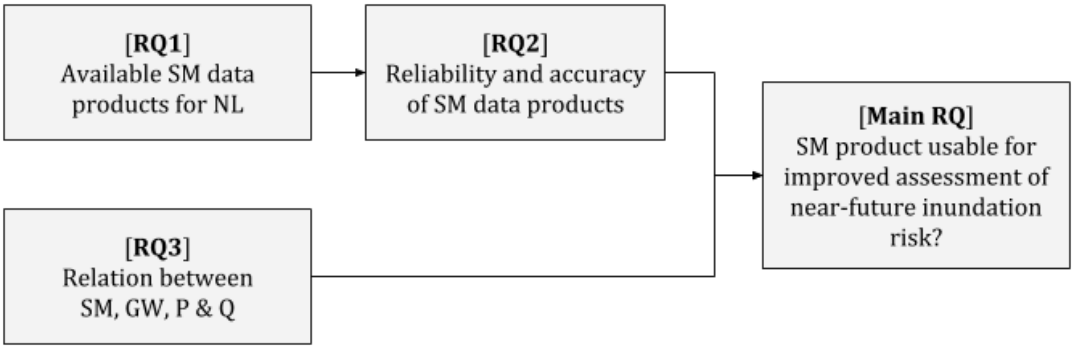

Figure 1.1 Diagram showing the connections and flow between the research questions. *SM: soil moisture, NL: the Netherlands, GW: groundwater, P: precipitation, Q: discharge*.

2
Theory

In this chapter the basics of soil moisture are presented, followed by a word on in-situ methods for soil moisture estimation. The latter part of this chapter describes remote sensing methods for soil moisture estimation, followed by data assimilation techniques and rainfall-runoff modeling.

2.1 Soil Moisture

After precipitation has fallen on the land surface, part is re-evaporated, part may directly flow to the surface water in the process of overland flow, and part will infiltrate into the soil. Between the land surface and the groundwater table, pores in the soil contain both air and water (Figure 2.1). This zone is known as the unsaturated zone. The water stored in this zone is called soil water or soil moisture (SM). Once soil water reaches the unsaturated zone, it may return to the surface vertically through evaporation, or horizontally through soil water flow into the surface water. Alternatively, soil water will percolate from the unsaturated zone into the deeper groundwater (Figure 2.2). Soil water is considered important in many processes. The relation between soil water, plants, and the atmosphere is key for agricultural practices and is important in relation to climate change effects. Soil water is also important for the recharge of groundwater reservoirs. Less noticeable, but nonetheless important for specific situations, soil water provides a first defense against groundwater pollution (Hendriks, 2010).

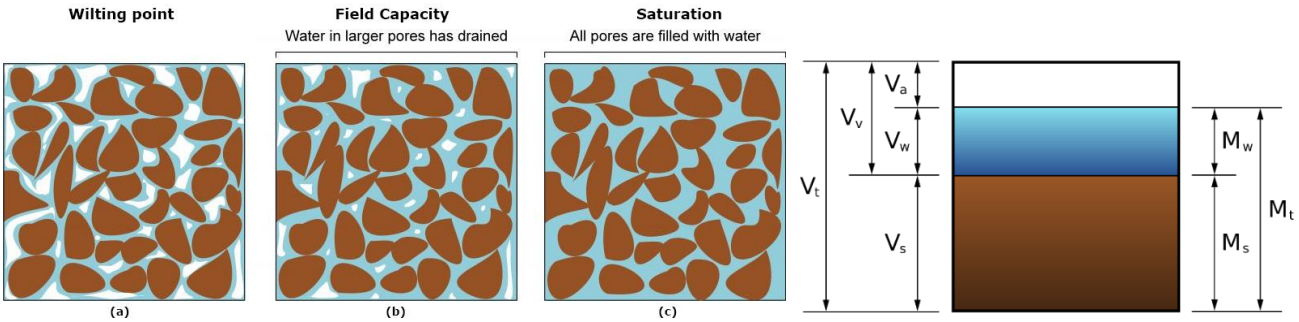

Figure 2.1 **[a-c]** soil moisture in the vadose zone at various degrees of saturation. **[d]** phase diagram showing soil composition. V is for *volume*; M is for *mass*. Subscripts s, w, and a stand for *soil*, *water*, and *air,* respectively. Subscripts v and t stand for *voids* and *total* respectively (source: Sjhan81 / CC BY-SA).

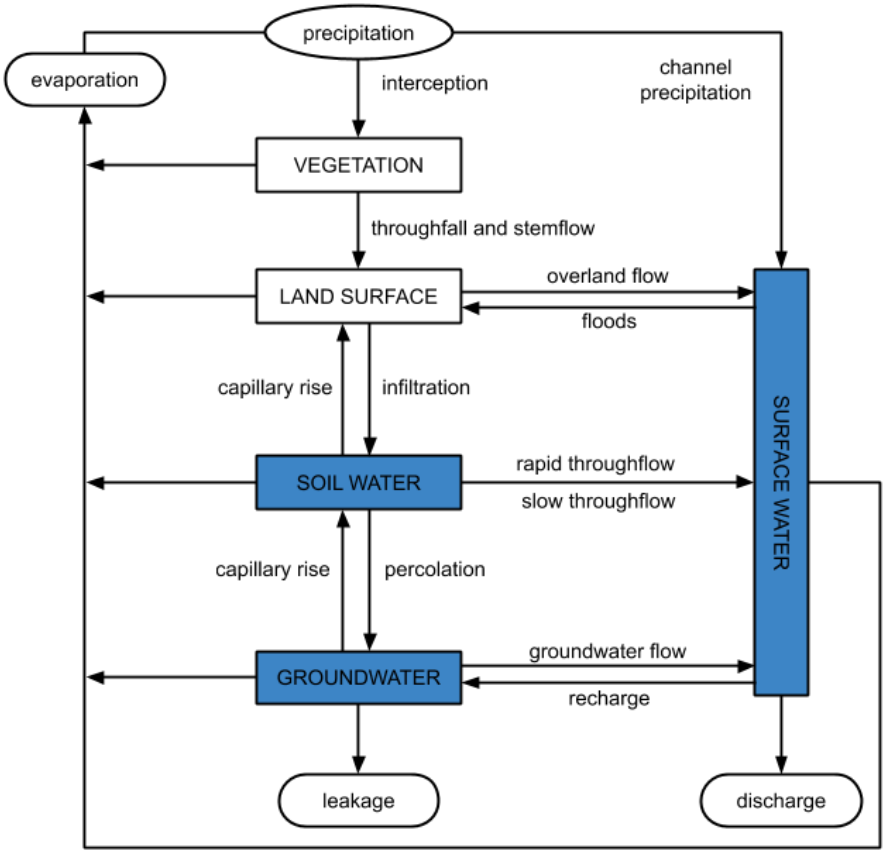

Figure 2.2 Drainage basin hydrological system (simplified). Ovals represent input/output processes; lower-case labels represent hydrological processes; rectangles represent water storages; the blue background shows the major types of water storages (for average conditions) (adapted from: Hendriks, 2010, p. 269).

The amount of soil moisture in the unsaturated zone is expressed on a gravimetric or volumetric basis (Bilskie, 2001). Gravimetric water content (θg) is defined as the mass of water per mass of dry soil. It is measured by weighing a soil sample before (m_t) and after (m_s) oven-drying and relating the obtained values [Eq. 2.1]. Volumetric water content (θ) of a soil is the volume fraction ($0 < \theta < 1$) or volume percent ($0 < \theta < 100\%$) of water-filled pores (V_w) per volume of soil (V_t) [Eq. 2.2]. Volumetric soil moisture as a fraction is used in this paper, unless otherwise noted.

$$\theta_g = \frac{m_w}{m_s} = \frac{m_t - m_s}{m_s} \qquad \text{[Eq. 2.1]}$$

$$\theta = \frac{V_w}{V_t} \ (\times 100\%) \qquad \text{[Eq. 2.2]}$$

Interaction between soil water and soil depends on the type of soil. Due to the fact that the soil material and pore size distribution differs per soil and because different forces may be at work, the relation between suction and volumetric moisture content differs per soil type. Sand consists of grains and the forces at work in the pore are mainly the capillary forces. Clays have a laminated structure and negatively charged surfaces that attract cations, such as Na^+ and Ca^{2+}, in the soil. Electrostatic forces bind the cations to the clay sheets and as a consequence the soil water holding the cations is also bound to the clay (Hendriks, 2010, p.152). The relation between suction and the volumetric moisture content (θ) is described by a soil moisture retention curve or pF curve (Figure 2.3).

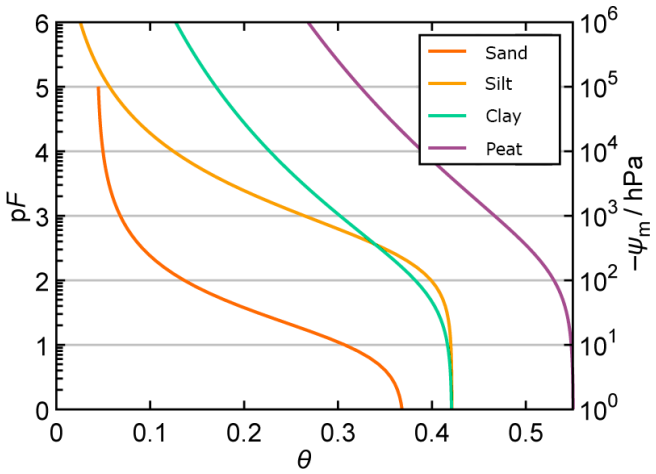

Figure 2.3 Example of water retention curves for sand, silt, clay, and peat soils. The horizontal and vertical axes denote the volumetric moisture content and the suction, respectively.

2.2 In-situ methods for soil moisture estimation

Various methods and devices exist to make soil moisture measurements, e.g. the feeling method, gravimetric method (by oven drying), tensiometers, electrical resistance blocks, time domain reflectometers, frequency domain reflectometers, capacitance probes, neutron probes (Evans & Sneed, 1991), or cosmic-ray scanners (Zreda *et al., 2012*). The gravimetric method is simple and reliable and is therefore often used for calibrating the other soil moisture sensing devices (Evans & Sneed, 1991).

All sensors used during this thesis research are based on the dielectric constant method. Therefore, only that method will be further explained.

Dielectric constant method

The dielectric constant method measures the capacity of a non-conductor (in this case: soil) to transmit high frequency electromagnetic waves or pulses. By calibration, the obtained values are related to the soil moisture content. This method is based on the fact that dry soil has a low dielectric value (~2 to 5), compared to a very high value for water (80 to 90, measured between 30 MHz and 1GHz). As the water content in the water-soil mixture increases, the dielectric constant increases. An important limitation of the method is that the measured dielectric constant of the soil mixture drops considerably as water in the soil becomes ice (van der Velde *et al.*, 2019) (Figure 2.4). One specific dielectric constant method (used during the research) is *capacitance* in which a sensor uses the soil as a capacitor element and uses the 'soil charge-storing capacity' to relate the measurement value to water content. Alternative dielectric constant methods are *time-domain reflectometry* and *frequency-domain reflectometry.*

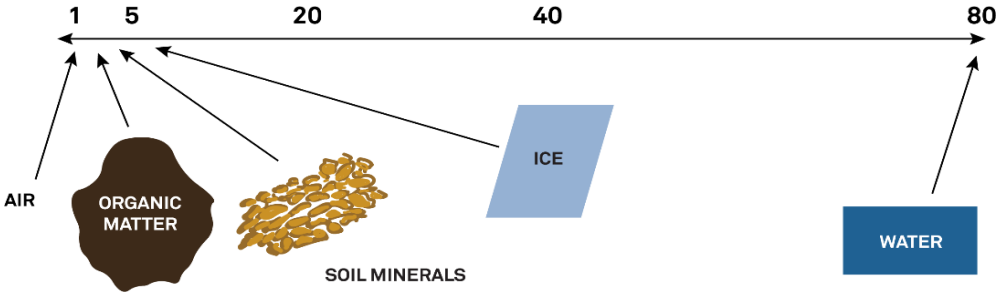

Figure 2.4 Typical dielectric constants (capacity to store charge) for common solids, liquids, and gases (METER Group, n.d.).

2.3 Remote sensing methods for soil moisture estimation

A multitude of literature has shown that remote sensing data can be used to give estimates of environmental variables and fluxes (Moradkhani, 2008; Reichle, 2008; Ma *et al*., 2015; STOWA, 2016; Zhuo & Han, 2016; Sadeghi *et al*., 2018). The growing extent of high-resolution remote sensing soil moisture products has created possibilities for integrating soil moisture data in water management approaches (Entekhabi *et al*., 2010; Petropoulos et al., 2015; Benninga *et al*., 2019).

The sensors or instruments used in remote sensing practices may either use the sun as their source of energy (passive) or supply their own source of energy (active), measuring the amount of energy that is reflected (Figure 2.5).

Technological progress in satellite remote sensing has shown that soil moisture can be measured by a variety of remote sensing techniques, including optical, thermal, passive- and active microwave measurements. Each method with its own strengths and weaknesses (Table 2.1).

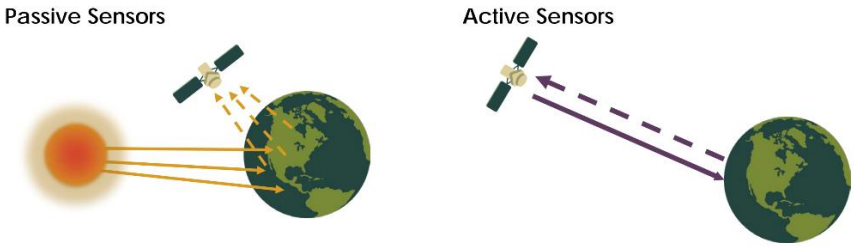

Figure 2.5 Diagram of a passive sensor versus an active sensor (Applied Remote Sensing Training, n.d.).

Table 2.1 Summary of remote sensing techniques for near-surface soil moisture estimation (Wang & Qu, 2009).

Spectrum domain		Properties observed	Advantages	Limitations
Optical		Soil reflection	Fine spatial resolution Broad coverage	Limited surface penetration Cloud contamination Many other noise sources
Thermal infrared		Surface temperature	Fine spatial resolution Broad coverage Physically well understood	Limited surface penetration Cloud contamination Perturbed by meteorological conditions and vegetation
Microwave	Passive	Brightness temperature Dielectric properties Soil temperature	Low atmospheric noise Moderate surface penetration Physically well understood	Low spatial resolution Perturbed by surface roughness and vegetation
	Active	Backscatter coefficient Dielectric properties	Low atmospheric noise Moderate surface penetration High spatial resolution Physically well understood	Limited swath width Perturbed by surface roughness and vegetation

Microwave remote sensing for soil moisture estimation

The microwave region of the electromagnetic spectrum ranges in wavelength (λ) from 1 mm to 100 cm. Microwave remote sensing allows for measurements under most weather conditions and at any time of the day. Depending on the wavelengths involved, microwave energy can penetrate through haze, light rain and snow, clouds, and smoke (Lillesand *et al*., 2000, p.638).

Radar (*radio detection and ranging*) is a form of active microwave sensing. Radar works by transmitting pulses of microwave energy in the direction of interest and recording the strength and origin of backscatter received from objects within the system's field-of-view (Lillesand *et al*., 2000, p.639).

Two primary factors that influence the transmission characteristics of radar signals are the wavelength and the polarization of the energy pulse used (Lillesand *et al*., 2000, p.659). In soil moisture estimation C-band measurements (λ=3.75-7.5 cm, f=8-4 GHz) and L-band measurements (λ=15-30 cm, f=2-1 GHz) are common. Soil moisture and surface wetness conditions become particularly apparent at longer wavelengths (Lillesand *et al.*, 2000, p.676). Table B.1 in Appendix B shows a full list of common wavelength bands for radar.

Depending on the wavelength and the surface roughness, a radar pulse may either backscatter or reflect (Figure 2.6). Reflected signals are not captured by the sensor. A modified Rayleigh criterion typifies the surface roughness based on the root-mean-squared surface height variation, the wavelength, and the local incidence angle (θ) (Equations 2.3 & 2.4) (Sabins, 1997). Generally, shorter wavelengths are more easily backscattered than longer wavelengths. For L-band measurements, a surface variation of >1.00-2.75 cm will generally be classified as intermediate and >5.68-15.6 cm will be classified as rough (i.e. good backscatter), depending on incidence angle (Table B.2 in Appendix B).

smooth: $$h\,(RMS) < \frac{\lambda}{4.4\cos\theta}$$ [Eq. 2.3]

rough: $$h\,(RMS) > \frac{\lambda}{25\cos\theta}$$ [Eq. 2.4]

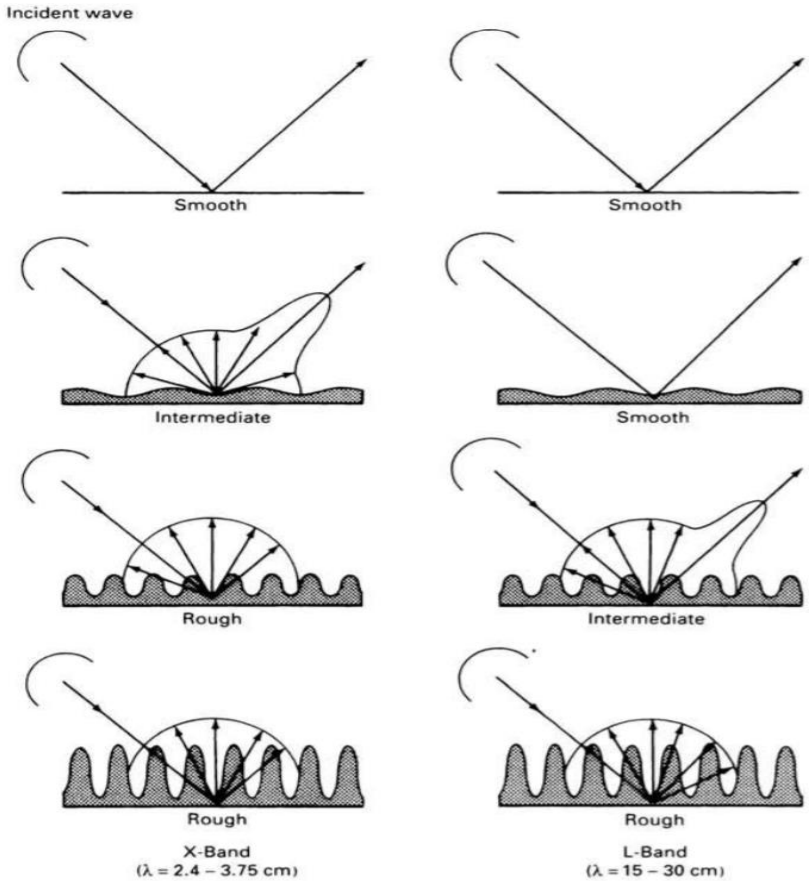

Figure 2.6 X-band and L-band radar reflection from surfaces of varying roughness (top-to-bottom: <0.10, 0.5, 1.5, >10.0 cm). (Lillesand *et al*., 2000, p.670).

Microwave soil moisture measurements rely on the large contrast between the dielectric properties of water (~80) and soil particles (<4). As moisture content increases, the dielectric constant of the soil-water mixture increases, and this change can be detected by microwave sensors (Njoku & Kong, 1977; Dobson *et al*, 1985). Penetration of radar waves is normally limited to depths of a few centimeters, especially when soil moisture is present (Lillesand *et al*, 2000, p.676). It is generally believed that the penetration depth is about one-third of the wavelength (Schmugge, 1985), which is about 1-2 cm for the C-band and 6-7 cm for the L-band.

Freezing and thawing processes, and the presence of frozen ground or wet snow, may impact the microwave backscatter measurements. Therefore, they have a negative effect on remote sensing soil moisture retrieval (Zwieback *et al.*, 2015).

Passive microwave remote sensing

Although operating in the same spectral region as radar, passive microwave systems do not supply their own source of illumination but measure the naturally present microwave energy within the field-of-view. Blackbody radiation theory is central to the concept of passive microwave sensing. Most passive microwave systems operate in the same spectral region as the shorter wavelength radar ($\lambda \leq 30$ cm). This region is the low-energy tail of a 300 K blackbody radiation curve, typifying terrestrial features (Figure 2.7). In this spectral region, all objects or surfaces in the natural environment emit microwave radiation, but very faintly compared to the visible or infrared spectrum (Lillesand *et al*, 2000, p.720). The relatively low amount of microwave energy available to passive satellite sensors requires large fields-of-view to collect sufficient energy for a measurement. The amount of emitted radiation is related to the temperature and dielectric properties of the topsoil (Lopez-Baeza, 2012).

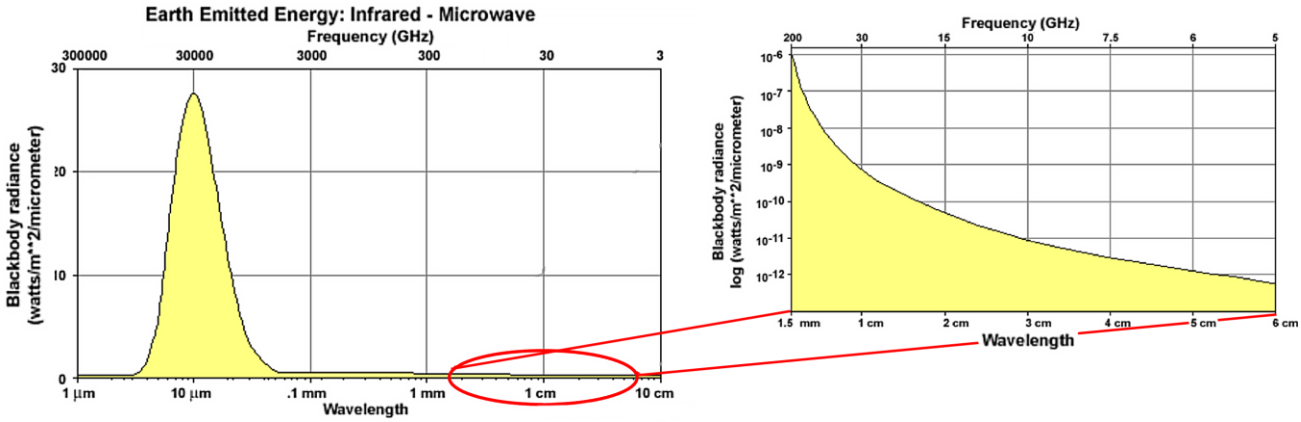

Figure 2.7 Earth emitted energy. Right panel shows the (passive) microwave spectral region (adapted from Lopez-Baeza, 2012).

2.4 Soil moisture data products (data assimilation)

A drawback of in-situ soil moisture measurements is that they are usually not representative for larger areas, because soil moisture can be highly variable at various spatial scales (Wang & Qu, 2009). Adequate in-situ sampling of larger areas is often unfeasible (for example due to high costs). To obtain the state of soil moisture on a larger scale, one could use either a model or remote sensing data. However, a modeled estimate is subject to errors originating from simplifications and assumptions. Model input uncertainties may also increase the uncertainty (e.g. imperfect forcing data and uncertain model parameters) (TU Delft, n.d.). Despite the advantages of remote sensing, such as high spatial coverage, it is also not ideal. Horizontal coverage may be high, but vertical distribution may be limited, e.g. only the top few centimeters are measured, while the interest is often in the rootzone or the full unsaturated zone. Furthermore, remote sensing observations may be indirect in the sense that the quantity of interest might not be directly measured but is rather the result of a conversion of for example the backscatter or brightness temperature that is recorded by the sensor.

To overcome the limitations of both individual methods, data assimilation is often used. This is a method in which models and (remote sensing) observations are combined, in order to obtain an estimate of soil moisture conditions that is better than the estimate as obtained from only the individual models or the observations. The soil moisture data products in this thesis are based on such assimilation methods. The exact structure differs per soil moisture product and is therefore described per product in Chapter 4.1.

2.5 Rainfall-runoff models

A rainfall-runoff model is a representation of the part of the water cycle that concerns the surface runoff of a hydrologic catchment area. Such models are generally used to understand runoff processes and to make discharge predictions for water management practices or to design hydraulic engineering measures for flood control. The complexity of runoff models varies broadly. The most basic models (e.g. metric models) estimate discharge based on observations, without characterizing the various hydrologic processes involved (Kokkonen & Jakeman, 2001). Conceptual models use (simplified) mathematical conceptualization of the system, usually by modelling a number of interconnected storages that represent the components of the hydrological process through recharge and depletion (Jaiswal *et al*, 2020). Conceptual models are usually lumped in nature, which means that the same parameter values are used for the full catchment, thus ignoring the spatial variability of parameters. Physical models are more complex and represent hydrological processes through mass, momentum, and energy conservation equations. Physical models account for the variability of land use, slope, soil, and climate to deal with the hydrological processes within the watershed (Jaiswal *et al*, 2020). Physical models usually require large amount of data and much computational power.

3

Methods and data

3.1 Study site description

The research focused on the province of North Brabant (Noord-Brabant) in the Netherlands, more specifically the management areas of the water authorities Brabantse Delta and Aa en Maas (Figure 3.1). These areas were chosen because the research internship took place at Brabantse Delta, but there was a better historic data availability for the area of Aa en Maas, especially in terms of soil moisture data.

Waterschap Brabantse Delta

The management area of water authority Brabantse Delta (WSBD) comprises the part of the province of North Brabant that lies to the west of the line Waalwijk / Baarle-Nassau and to the south of the Hollandsch Diep, the Amer and the Bergsche Maas. This area covers ~1707 km². The surface level in the northern half of WSBD is generally within -1 to +1 m NAP (Amsterdam Ordnance Datum). The physical geography consists of marine clays in the north-west and fluvial clays in the north-east. In the southern half, below the line Bergen op Zoom – Breda, the terrain is made up of sandy high grounds varying between a couple of meters and 20-35 m +NAP.

Waterschap Aa en Maas

The management area of water authority Aa en Maas (WSAM) is located (north)east of Brabantse Delta, it covers ~1610 km². In the far north of WSAM the physical geography consists of a narrow band (<10 km horizontally) of fluvial clays and the surface level is generally below 10 m +NAP. The central and southern areas consist of sandy high grounds, with a surface level that varies between a couple of meters and 25-40 m +NAP.

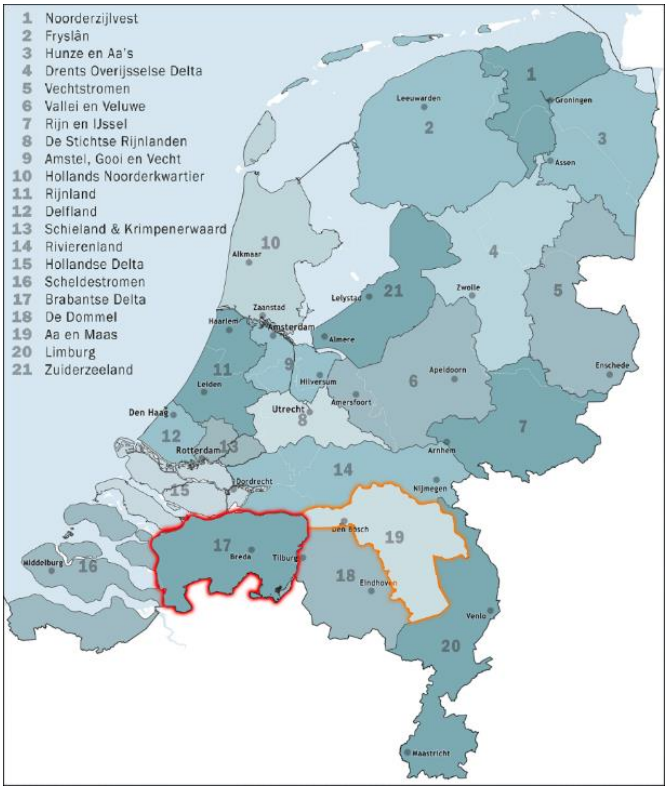

Figure 3.1 Map of the Netherlands showing the regional water authorities. Brabantse Delta and Aa en Maas are outlined in red and orange, respectively (adapted from: Janwillemvanaalst / CC BY-SA).

3.2 Available soil moisture data products for the Netherlands

An overview of the operational (remote sensing) soil moisture data products for the Netherlands was made from literature research and existing knowledge of the cooperating water authorities Brabantse Delta and Aa en Maas. Literature research was done through search engines, using applicable keywords in English and Dutch (soil moisture, remote sensing, product, Netherlands // bodemvocht, satelliet, Nederland; etc.). In cases where company websites showed only a brief notice about a possible soil moisture data product, those companies were contacted for further clarification.

The main interest was to find soil moisture data products that are ready for use by an end-user and that are also of high spatial resolution (preferably less than a few hundred meters per pixel, but at least less than a few kilometers). For completeness, the overview was supplemented with 'source' satellite products (e.g. SMAP, AMSR-E, Sentinel). Those are satellites which are often used as a source of input data for the end-user products.

The properties describing the products are given in Appendix A. That includes the type of product (source or end-user product), origin of the source data (for end-user products), spatial resolution, spatial extent, temporal resolution, and sensing depth. These properties were obtained through search engines, product websites, digital product brochures, webinars, and personal communication. The end-user products of which the (output) data was available for the thesis research are further described in the results section, including previous validation results of the product to in-situ measurements.

3.3 In-situ soil moisture measurements

In-situ soil moisture measurements were obtained from field sensors that were pre-installed in at 18 sites throughout the province of Noord-Brabant, of which 2 are located in the WSBD area and 16 are located in the WSAM area (of which 15 in the Raam catchment (Benninga *et al*, 2018) and 1 at de Bult) (Table 3.1 & Figure 3.2).

Time period

In the WSBD area, measurements were available from 7-1-2020 till 22-4-2020. For de Bult area, measurements were available from 14-9-2017 to 8-5-2018. For the Raam catchment soil moisture measurements were available from 5-4-2016 till 5-04-2019.

Sensor models

The WSBD sensors were of the model METER® TEROS 10, the sensors used in the Raam catchment (WSAM) were of the model Decagon® 5TM, and the sensor at de Bult (WSAM) was a Decagon® EC5 (Table 3.2).

Pre-processing of in-situ measurements

The measurements varied between the water authorities (and catchments) in terms of time interval, measurement depths and the number of sensors per site. The timeseries were homogenized by converting to daily-average values of soil moisture. For WSBD, the sensors were installed as a doublet at each depth. The doublet measurements were averaged into a single soil moisture value.

Table 3.1 Overview of in-situ soil moisture sites, including coordinates, model, and time frame.

ID	x-coordinate (RD new)	y-coordinate (RD new)	Model	Time frame
WSBD_Bavel	115619	398494	METER TEROS 10	7-1-2020 – 22-4-2020
WSBD_Rijsbergen	104197	392584	METER TEROS 10	7-1-2020 – 22-4-2020
WSAM_Bult	186508	390081	Decagon EC5	14-9-2017 – 8-5-2018
WSAM_Raam_01	178746	416080	Decagon 5TM	5-4-2016 – 5-4-2019
WSAM_Raam_02	174576	410701	Decagon 5TM	5-4-2016 – 5-4-2019
WSAM_Raam_03	177267	411515	Decagon 5TM	5-4-2016 – 5-4-2019
WSAM_Raam_04	177863	413975	Decagon 5TM	5-4-2016 – 5-4-2019
WSAM_Raam_05	174047	412930	Decagon 5TM	5-4-2016 – 5-4-2019
WSAM_Raam_06	182348	414484	Decagon 5TM	9-5-2016 – 5-4-2019
WSAM_Raam_07	188281	412613	Decagon 5TM	9-5-2016 – 5-4-2019
WSAM_Raam_08	184089	396122	Decagon 5TM	9-5-2016 – 5-4-2019
WSAM_Raam_09	181516	400101	Decagon 5TM	5-4-2016 – 31-1-2018
WSAM_Raam_10	179978	405124	Decagon 5TM	5-4-2016 – 5-4-2019
WSAM_Raam_11	189582	400334	Decagon 5TM	5-4-2016 – 5-4-2019
WSAM_Raam_12	185453	405695	Decagon 5TM	5-4-2016 – 5-4-2019
WSAM_Raam_13	189261	406406	Decagon 5TM	5-4-2016 – 5-4-2019
WSAM_Raam_14	186824	409720	Decagon 5TM	5-4-2016 – 5-4-2019
WSAM_Raam_15	182681	412176	Decagon 5TM	5-4-2016 – 5-4-2019

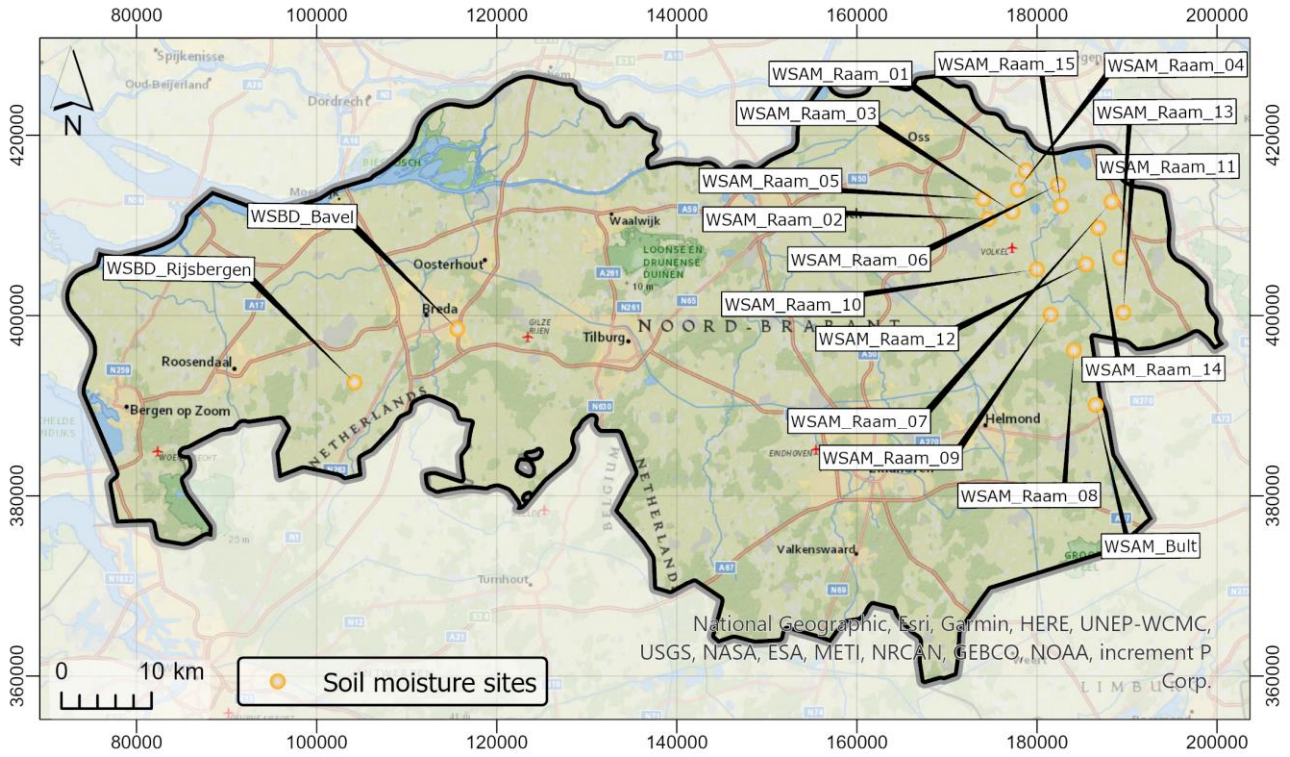

Figure 3.2 Soil moisture sensor locations in the province of Noord-Brabant, the Netherlands.

Table 3.2 Soil moisture sensor technical specifications. *Type: C = capacitance.*

Brand	Model	Type	Operating frequency	Range [m³/m³]	Resolution [m³/m³]	Accuracy
Decagon	5TM	C	70 MHz	0.00–1.00	0.0008 (from 0 to 50 VWC)	• Using Topp equation: ±0.03 m³/m³ typical in mineral soils that have solution EC <10 dS/m. • Medium specific calibration: ±0.02 m³/m³ in any porous medium.
Decagon	EC5	C	70 MHz	0.00–1.00	0.001	• Generic calibration: ±0.03 m³/m³ typical in mineral soils that have solution EC <8 dS/m. • Medium specific calibration: ±0.02 m³/m³ in any porous medium.
METER	TEROS 10	C	70 MHz	0.00–0.64	0.001	• Mineral soil calibration: ±0.03 m^3/m^3 typical in mineral soils that have solution EC <8 dS/m. • Medium specific calibration: ±0.01–0.02 m^3/m^3 in any porous medium.

3.4 Correlation of remote sensing products to in-situ measurements

In order to compare the remote sensing products to the in-situ measurements, Pearson and Spearman correlations between the two were calculated. The correlation coefficient is a statistical measure for the strength of the link between two sets of data. In general, the result of the method can range from 1.0 (a perfect positive correlation) to -1.0 (a perfect negative correlation). A correlation of 0 indicates that there is no association between the two sets of data. A description of different correlation values is given in Table 3.3. Due to the nature of all products used in this research, e.g. increasing value as soil moisture increases, only positive correlation values are assumed to be realistic. The **Pearson correlation** (denoted as R) measures a linear dependence between two variables, also known as a *parametric correlation*. The **Spearman correlation** (denoted as ρ (rho)) is a non-parametric measure of rank correlation (statistical dependence between the rankings of two variables). It assesses the relationship between two variables using a monotonic function, which is a function that is entirely increasing or entirely decreasing; this function can be linear or non-linear.

For OWASIS the correlation was calculated for all sites, at an in-situ depth of 15-20 cm-surface (Raam: 20 cm; de Bult and WSBD: 15 cm). Correlations between VanderSat and in-situ soil moisture were calculated only for the WSAM sites, at a depth of 5 cm below surface level. The VanderSat product was not available for the WSBD area. These depths were chosen because the VanderSat product measures the top 1-5 cm of the soil, while the OWASIS product models the rootzone (first tens of cm below surface level, depending on location). It was therefore assumed that the soil moisture measurements at 15-20 cm depth would better fit to OWASIS compared to the measurements at 5 cm depth.

Table 3.3 The strength of a correlation.

Value of coefficient (positive or negative)	Description
0.00 to 0.19	Very weak correlation
0.20 to 0.39	Weak correlation
0.40 to 0.69	Moderate correlation
0.70 to 0.89	Strong correlation
0.90 to 1.00	Very strong correlation

Correlation at single cell *and at* 3x3 grid

The correlations were made at different spatial scales of the remote sensing products: a single raster cell, the spatial average of multiple cells, and the spatial average at catchment scale. The first may be regarded as a very local scale and the latter as a regional scale correlation.

As a first indication of the correlation between in-situ measurements and the RS products, the timeseries of in-situ soil moisture measurements (15-20 cm depth) were compared to 'point data' (single cell) of the RS products. From the RS products the grid cell was used that contained the geographical location of the soil moisture sensor (Figure 3.3).

In an attempt to mitigate adverse effects of sometimes large cell to cell variation in the OWASIS product (see Discussion), the *single cell* correlation was supplemented with a *3x3-grid* version, in which the value of the OWASIS product was averaged over a 3x3 spatial grid (i.e. 9 cells) instead of just the single cell that contained the soil moisture sensor (Figure 3.3). This method was not applied to VanderSat data, because no unrealistic cell to cell variation was found for that product.

The OWASIS product was also correlated to the in-situ measurements on a calendar month basis, i.e. all measurements of January (of available years) were grouped and correlated, all measurements of February, etc. For the WSBD sites this only includes the months January through April of the year 2020, as no further data was available.

Furthermore, it was researched whether any differences in correlation between the soil moisture sites could be explained by the site characteristics, e.g. geographic location, soil type (BOFEK2012), land-use type (agricultural or non-agricultural).

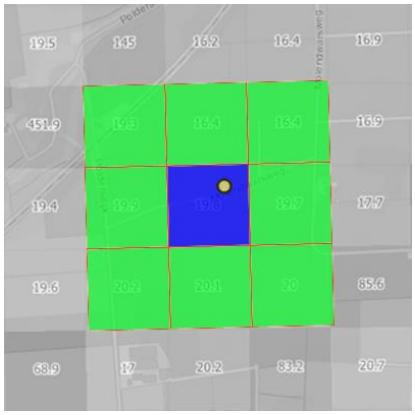

Figure 3.3 Example of a spatial grid indicating a soil moisture sensor location (yellow), the coinciding cell (blue) and a 3x3 grid (green).

Correlation at catchment scale

The *single cell* and *3x3-grid* correlations only provide information on a very local scale and may be subject to errors due to the high spatial variability of soil moisture. Regardless of the quality of those correlations, the quality may be very different when correlating soil moisture at the scale of a catchment. The RS products were averaged over the extent of the Raam catchment; an area of approximately 20 km by 20 km (~223 km²) (Figure 3.4). The in-situ soil moisture measurements were averaged over all sites that were within the extent of the catchment (WSAM_Raam_01 through 07,10,12,13,14,15).

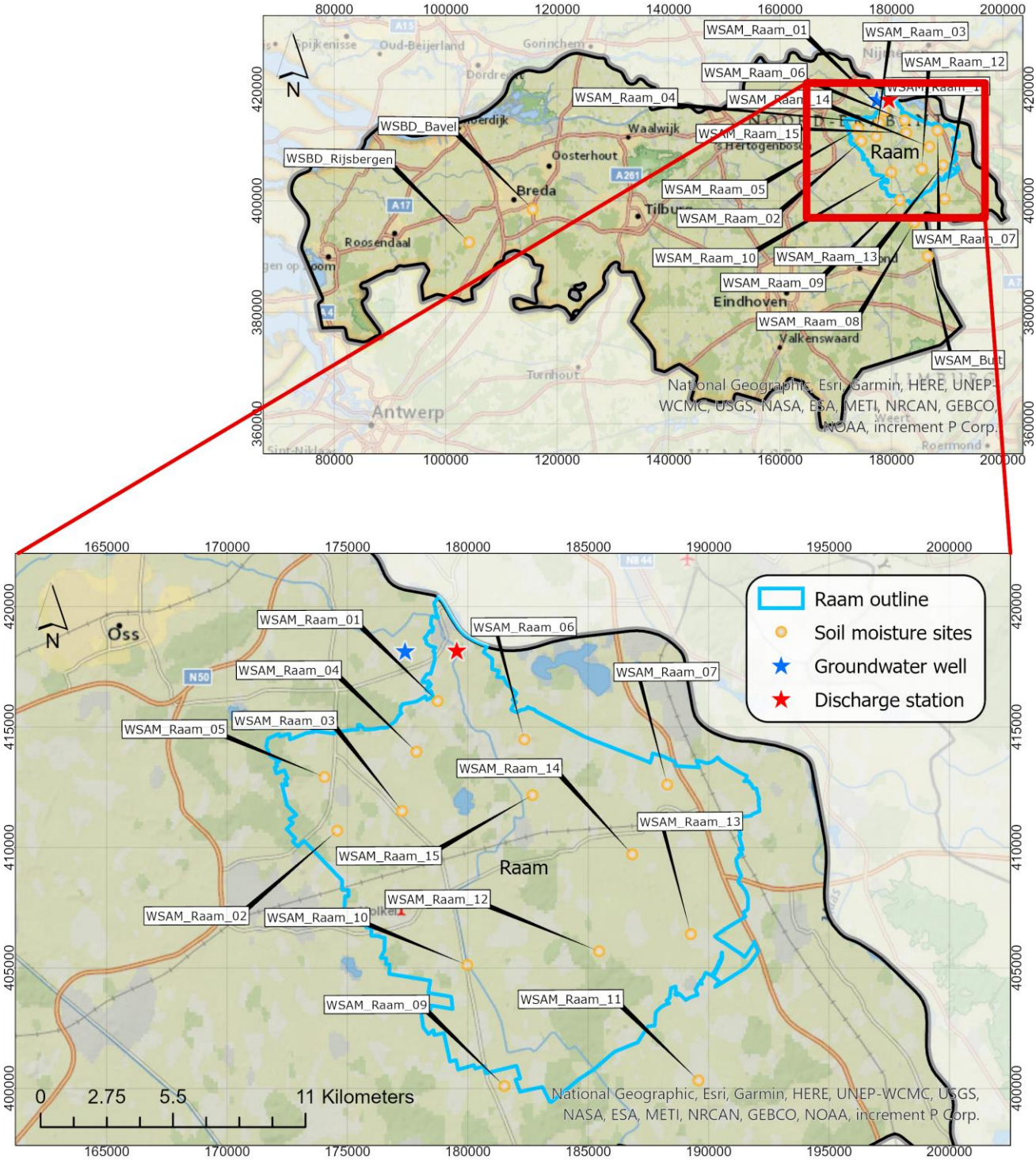

Figure 3.4 Map indicating the outlines of the Raam catchment and the soil moisture sites, groundwater and discharge measurement locations.

3.5 Relation between precipitation, soil moisture, groundwater level and discharge

A simple rainfall-runoff analysis was used to investigate the extent to which the state of soil moisture can be used in inundation-risk assessment. The analysis was used to show how soil moisture state and groundwater level affect runoff generation in the study area. The analysis was based on observations only and disregarded the hydrological processes between precipitation and discharge (except for soil moisture and groundwater levels)[2]. Daily precipitation, soil moisture content, groundwater levels and discharge measurements of the Raam catchment were obtained for the period 15-02-2017 - 01-04-2019.

Precipitation data was obtained from the '*HydroNET Neerslagradar*' over the Raam catchment. Discharge was measured at the town of Grave (discharge measurement station ADM108, x=179545, y=418180) just before the Raam enters the river Meuse in the north of the catchment. The observed daily average discharges [in m^3/s] were converted to [mm/day] by multiplying by the average number of seconds in a day (86,400) and dividing by the catchment area (approximately 121.3 km^2). The soil moisture state was based on the Raam catchment average of the in-situ measurements (n=12 sites, shown within the blue outline in Figure 3.4). Groundwater levels were measured approximately 2 km west of the discharge station, near the town of Velp (NITG-code: B45F0281001, x=177398, y=418155). The surface level at the groundwater monitoring well is situated at 8.4 m +NAP.

The relationships between precipitation, soil moisture state, groundwater level and daily discharge were made clear by creating two scatterplots. On one axis the daily precipitation was plotted [mm/day], on the other axis the daily discharge [mm/day]. The observed precipitation-discharge pairs were grouped into three classes of color-coding: red for relatively dry conditions, blue for relatively wet conditions, and grey in between. In one plot the color coding indicates the state of the soil moisture. In another plot the color indicates the groundwater depth. Division of classes was done automatically as the minimum-maximum range of observed soil moisture (for the first plot) and groundwater depth (for the second plot) divided by the number of classes (n=3).

[2] The simple analysis was used as an alternative to a conceptual model which turned out inapplicable, as described in the Discussion (section 5.1).

4 Results

4.1 Available soil moisture data products for the Netherlands

The soil moisture data products that are available for the Netherlands are categorized into *source satellite products* and *end-user products*. An overview of the properties of each product is provided in Appendix A. The source satellite products are not suitable for operational use at the water authorities, because they have to be further processed. Only the end-user products are elaborated in this chapter, which are OWASIS and VanderSat.

4.1.1 OWASIS soil moisture product

OWASIS offers information at 250 m resolution for the whole of the Netherlands about the historical, actual, and short-term forecasted soil storage capacity and water availability. OWASIS was developed by HydroLogic in cooperation with ESA, STOWA, WUR, eLEAF, and Rijkswaterstaat. The product became operational on 01-01-2018. OWASIS combines various data sources into products of soil storage capacity and water availability (Figure 4.1). This is done by feeding the inputs into a water balance solver, which is the *Landelijk Hydrologisch Model* (Dutch National Hydrologic Model, LHM). The LHM is a set of models that compute the state of the unsaturated and saturated zones in a detailed way. The output consists of the available water storing capacity of the soil, the amount of soil moisture, and modeled groundwater levels. These outputs are made available through the HydroNET-platform (webportal and FTP) (van den Brink *et al.*, 2019).

The core of the LHM is the Modflow+MetaSWAP model, which is a coupled model of Modflow (saturated zone / groundwater layering) and MetaSWAP (unsaturated zone) (Box 4.1). The main inputs are forcing data of precipitation and evapotranspiration, and the water levels in the main system (i.e. large rivers). Additional inputs consist of soil type, surface level, etc.). Although the model outputs on a daily basis, the water levels in the main water systems are updated into the model on a monthly basis. The up-to-date water levels are not always available, therefore the model may fall back on long-term averages, while still considering dry/wet years. For example, if the current year is a dry year, the historic long-term average of dry years is taken. The regional water systems in the model are fed with summer and winter levels under 'normal management'.

For historic dates, precipitation data is obtained from KNMI (Royal Dutch Meteorological Institute) radar data, but this radar data is then corrected based on KNMI rain gauges. This is done because radar is generally good in providing the spatial distribution, while rain gauges provide a better value for the actual amount of precipitation.

Until 2020 the actual evapotranspiration was based on the eLEAF-service. As of 2020 it is based on VanderSat's evapotranspiration service (*note: this is not the VanderSat soil moisture product as described further on in the research*). OWASIS itself is in essence only a model, but the actual evapotranspiration data (eLEAF / VanderSat) is the component that is based on remote sensing data. The LHM model was modified by HydroLogic to work with actual evapotranspiration data, because the standard LHM model (Modflow+MetaSWAP) uses reference crop evaporation and subsequently computes an estimation of the actual evapotranspiration.

The operational OWASIS service also provides forecast data up to three days ahead. In that case, precipitation is based on forecasts of the ECMWF weather model. Actual evapotranspiration is not available as a forecast; therefore, Makkink reference evapotranspiration (Box 4.2) is calculated based on forecast temperature, cloud cover and incoming radiation. Forecast actual evapotranspiration is then estimated by scaling the reference by a factor that is based on the actual evapotranspiration of the previous few days.

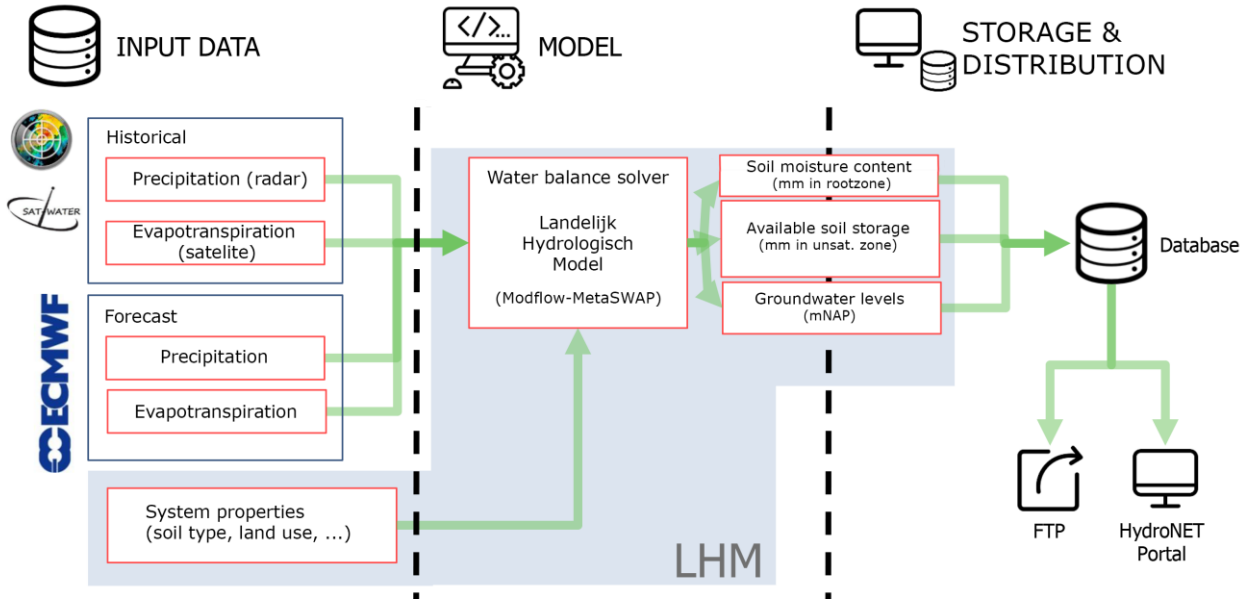

Figure 4.1 Overview of the OWASIS service (Adapted from Hydrologic, 2018, p.7).

Box 4.1 Modflow+MetaSWAP.

MetaSWAP is the model component in the LHM that describes the processes of the phreatic groundwater level, the unsaturated zone, and the exchange of the soil-plant-atmosphere system. The component is linked to MODFLOW, enabling metaSWAP to be used in a regional and national context (Toorn *et al.*, 2016). MetaSWAP simulates the processes from groundwater level to plant-atmosphere interactions. It is a so-called 'metamodel' of SWAP (Van Dam *et al.*, 2008). The meta concept is based on a simplified solution of the non-linear partial differential equation for describing soil physical processes, the so-called Richards equation. This equation is replaced by two 'ordinary' differential equations, one for the process description and one for the water balance (Toorn *et al.*, 2016). Upscaling to 'aggregation layers' is used in order to do so. Validation of the method is given in (van Walsum & Veldhuizen, 2011).

Box 4.2 Makkink method for evapotranspiration.

The Makkink method requires a measurement of the temperature and the global radiation to estimate evapotranspiration, according to the following formula:

$$\lambda E = 0.65 \frac{s}{s+\gamma} Kin$$

In which:

λE = latent heat flux (W m-2)
s = derivative of esat at air temperature T (kPa K-1)
γ = psychrometer constant (kPa K-1)
Kin = daily sum of global radiation (W m-2)

The assumptions for this method are that the soil heat flux can be neglected relative to the net radiation and that the net radiation is approximately half of the global radiation (Kin). Also, the impact of wind on evapotranspiration is assumed negligible. The first assumption is only valid for land areas and the second assumption is based on average summer conditions in the Netherlands (Feddes et al., 2003).

Validation of OWASIS

Soil moisture content and groundwater level forecasts from the LHM were validated over the year 2016, using soil moisture sensors at 15 locations in the province of North-Brabant (WSAM, Raam catchment) and 67 locations with groundwater monitoring wells in the province of Utrecht. Three versions of the LHM were compared: standard LHM, LHM ETref, LHM ETact (HydroLogic, 2018) (Table 4.2). Precipitation input for the

standard LHM is based on KNMI data, which is interpolated from 100-300 stations nationally, and evaporation data that is interpolated from 32 stations based on Makkink (Box 4.2). In the LHM ETref version, precipitation data is obtained from the HydroLogic precipitation product (HydroLogic, 2012), evaporation is (again) obtained from the KNMI. The LHM ETact version can be regarded as the current 'OWASIS' product. In this version, precipitation is obtained from the HydroLogic precipitation product, and evaporation is obtained from the eLEAF actual evaporation service (as of 2020: VanderSat), which are based on remote sensing data and the algorithms SEBAL (Bastiaanssen *et al.*, 1998) and ET-Look (Pelgrum *et al.*, 2010). These algorithms solve the energy balance at the Earth's surface.

HydroLogic concluded in their validation study (Figures 4.4, 4.5) that there were too few measurement locations, and too little variability in soil types, surface level height and groundwater depth (and possibly distance to surface water) to make good statements about the performance of the LHM with an imposed ETact. The in-situ soil moisture measurements had many missing timeseries, disputing the quality of the dataset. Overall, it was concluded that (on average) both the model fit (R^2) and the error (RMSE) improved with an imposed ETact (HydroLogic, personal communication).

Table 4.2 Variations of the LHM used in the validation of OWASIS (HydroLogic, 2018).
Note: there are indications that the label R^2 should actually be R, as explained in the description of Figure 4.4.

	Precipitation	Evaporation	R^2	RMSE (mm)
Standard LHM	KNMI (RD1) daily sum based on 300 stations	KNMI (EV24) Makkink based on 32 stations	0.59	-
LHM ETref	HydroLogic precipitation product	KNMI (EV24) Makkink based on 32 stations	0.57	42
LHM ETact	HydroLogic precipitation product	eLEAF actual evaporation (remote sensing)	0.82	36

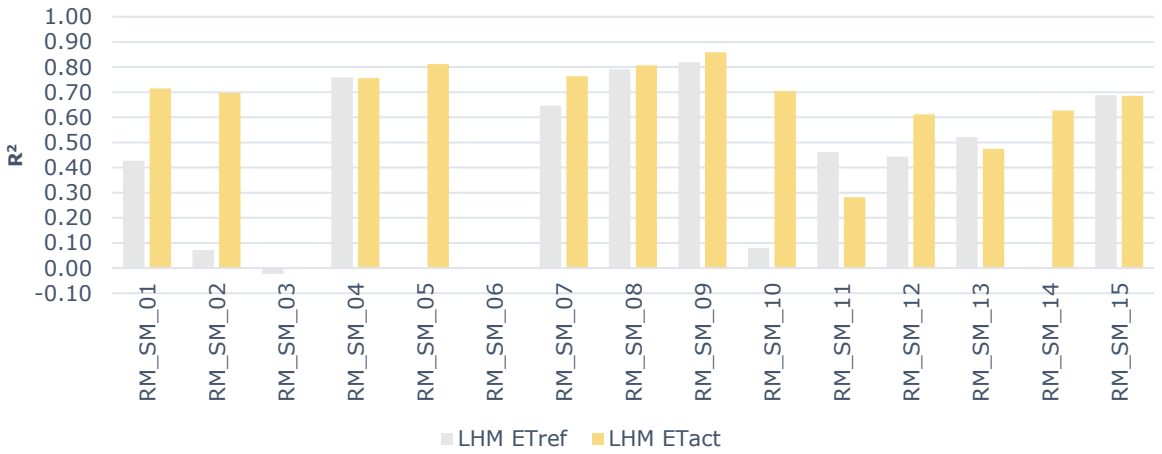

Figure 4.4 Correlation (R^2) of soil moisture in the rootzone: LHM vs in-situ, per location (source: HydroLogic).
Note: there are negative values in this graph (RM_SM_03), which should never be the case as R is squared. HydroLogic could not explain this error, but it is possible that the graph represents R rather than R^2 (personal communication).

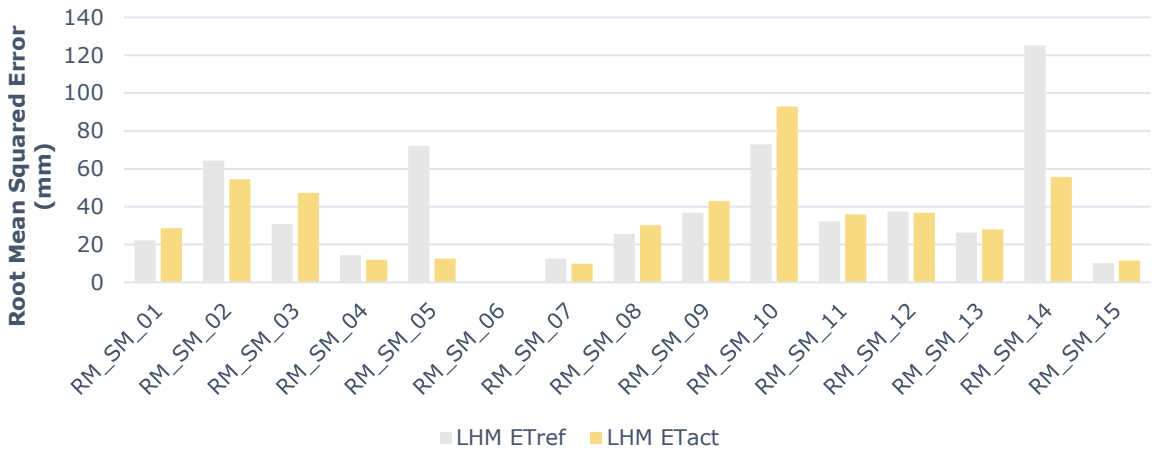

Figure 4.5 Root Mean Squared Error (RMSE) of soil moisture in the rootzone: LHM vs in-situ, per location (source: HydroLogic).

4.2.1 VanderSat L-band soil moisture product

VanderSat is a Dutch provider of global satellite-observed water and temperature data products. The VanderSat service uses passive microwave satellites (e.g. AMSR-E, AMSR-2, SMAP) which measure naturally radiating microwave signals from the Earth's surface. At the moment of writing, VanderSat uses nighttime observations during the satellites descending orbits (generally between 01:30 and 06:00 solar time). The measurements can be regarded as instantaneous and are representative for the time of overpass. Between 200 and 330 observations are expected per satellite, per year, depending on geographic latitude. The measured signal originates from the top layer of the soil. This can generally be up to 10 cm depth, with the strongest contribution from the uppermost layer. Commonly a depth of 5 cm is assumed, but in reality the penetration depth varies with moisture content. The measured depth is deeper if the soil is drier (VanderSat, n.d.). The precision of the soil moisture data is ~0.001 [m³/m³]. The accuracy is approximately 0.03 [m³/m³] (VanderSat, n.d.).

The VanderSat algorithm is based on the Land Parameter Retrieval Model (LPRM) (Owe *et al.*, 2008; De Jeu *et al.*, 2014; Van der Schalie *et al.*, 2017). In addition to this model VanderSat uses an algorithm to downscale the satellite-retrieved raw brightness temperature into a resulting soil moisture product of 100x100 m resolution. This downscaling yields a significant improvement over the original resolution (e.g. AMSR-2 C-band, at 62x35 km) (Figure 4.6) (VanderSat, n.d.). This downscaling process is technically relatively complex, but was well described by Mulder (2018): "By considering a Gaussian distribution inside the satellite footprint, it can be assumed that the center of a single footprint contributes more to the observed brightness temperature signal than the edges of that footprint. By using this Gaussian distribution, also footprints at for example 25% and 75% signal-intensity can be established, which results in footprints of different resolutions. Finally, by combining these different footprints, the geographical area of interest is overlain by multiple ellipses, in which pixels inside small footprints have larger weights than pixels inside large footprints. A high detailed land cover map is used to distinguish between land cover and open water. For each footprint that is overlaying the geographical area of interest, the percentage of land and water inside that footprint is determined. By using the percentage of land and water cover, and by using fixed brightness temperature values for pixels covering water, the brightness temperature values for each high-resolution land pixel can be calculated from the observed brightness temperature in the satellite footprint. The resulting high-resolution brightness temperature map is used as input in the Land Parameter Retrieval Model to calculate soil moisture […] at 100x100 m resolution. By downscaling the raw brightness temperature data instead of downscaling soil moisture, temperature and VOD, the method becomes more efficient, but also performs better around large water bodies such as lakes and along the coast (Figure 4.6)."

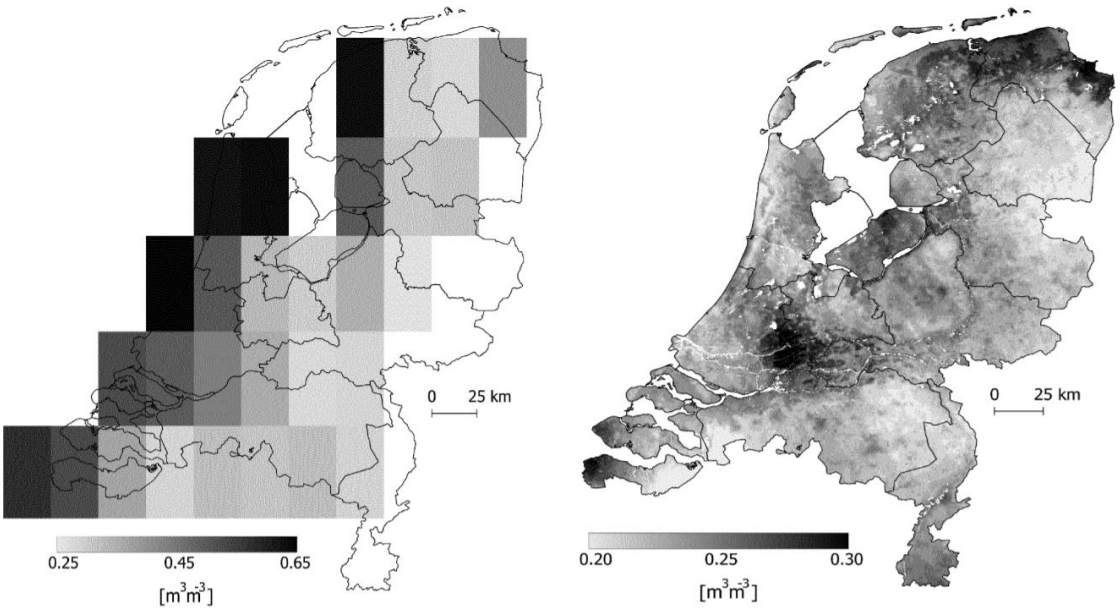

Figure 4.6 Soil moisture maps of the Netherlands, based on SMAP level 3 data with a resolution of 36 km (left), and based on the downscaling algorithm of VanderSat, resulting in a resolution of 100 m (right) (Mulder, 2018).

The analyses in this thesis research were done using version 1.0 of the VanderSat L-band soil moisture product (SM-LN_V001_100), which was released in January 2019. The current version is 3.0, which was released in September 2019. The newer version was not used in the research, because it was not available at the water authorities. The differences between versions can be found in the VanderSat release notes, at https://docs.vandersat.com/VanderSat_Release_Notes.html.

Validation of VanderSat

De Jeu & de Nijs (2017) calculated the correlation of two variations of the VanderSat product to both soil moisture and (phreatic) groundwater levels. One variation was based on AMSR-2 C-band and the other on SMAP L-band observations. Daily average soil moisture (at 3 cm depth) and groundwater levels at the KNMI monitoring site Cabauw (near Lopik) were used as in-situ data. Correlation coefficients of Pearson and Spearman were calculated (Table 4.3, Figure 4.7). Correlation values of generally over 0.75 were found. The L-band observations of SMAP performed slightly better than the C-band observations of AMSR-2, which may be due to the fact that L-band frequency generally has a larger penetration depth through vegetation, into the soil (Mulder, 2018). There was also a relatively strong correlation of in-situ soil moisture to groundwater levels (R=0.61–0.72).

Based on the results of Cabauw, the approach was upscaled to the full extent of the Netherlands by using the available groundwater level data from DINOloket. Focus was put on the Spearman correlation because the relationship between soil moisture and groundwater level was not always considered linear (de Jeu & de Nijs, 2017). Correlations of R ≥ 0.6 between remote sensing data and groundwater levels were found throughout the Netherlands, including the coastal areas and the Wadden islands. In total, 76% of all data pairs between soil moisture and groundwater level had a correlation >0.6 with SMAP and 54% with AMSR-2. Low correlations were found in areas where the relationship between topsoil moisture and groundwater level is strongly decoupled (de Jeu & de Nijs, 2017). The decoupling of soil moisture to groundwater with increasing depth is shown in (Figure 4.8).

Table 4.3 Statistics of the VanderSat products with respect to the soil moisture measurements at 3 cm and the measured groundwater levels at Cabauw. Statistics marked with an asterisk (*) are based on days for which all measurements were available between the period April 2015 and the end of March 2017 (adapted from: de Jeu & de Nijs, 2017).

	N	$R_{Pearson}$	$R_{Spearman}$	Time period
VanderSat (SMAP) vs SM	262 251*	0.81 0.81*	0.85 0.85*	April 2015 – March 2017
VanderSat (AMSR-2) vs SM	1533 251*	0.78 0.75*	0.85 0.81*	July 2012 – March 2017
VanderSat (SMAP) vs GW	271 251*	0.75 0.76*	0.80 0.81*	April 2015 – March 2017
VanderSat (AMSR-2) vs GW	1569 251*	0.78 0.75*	0.79 0.76*	July 2012 – March 2017
SM vs GW	1654 251*	0.68 0.61*	0.74 0.72*	July 2012 – March 2017

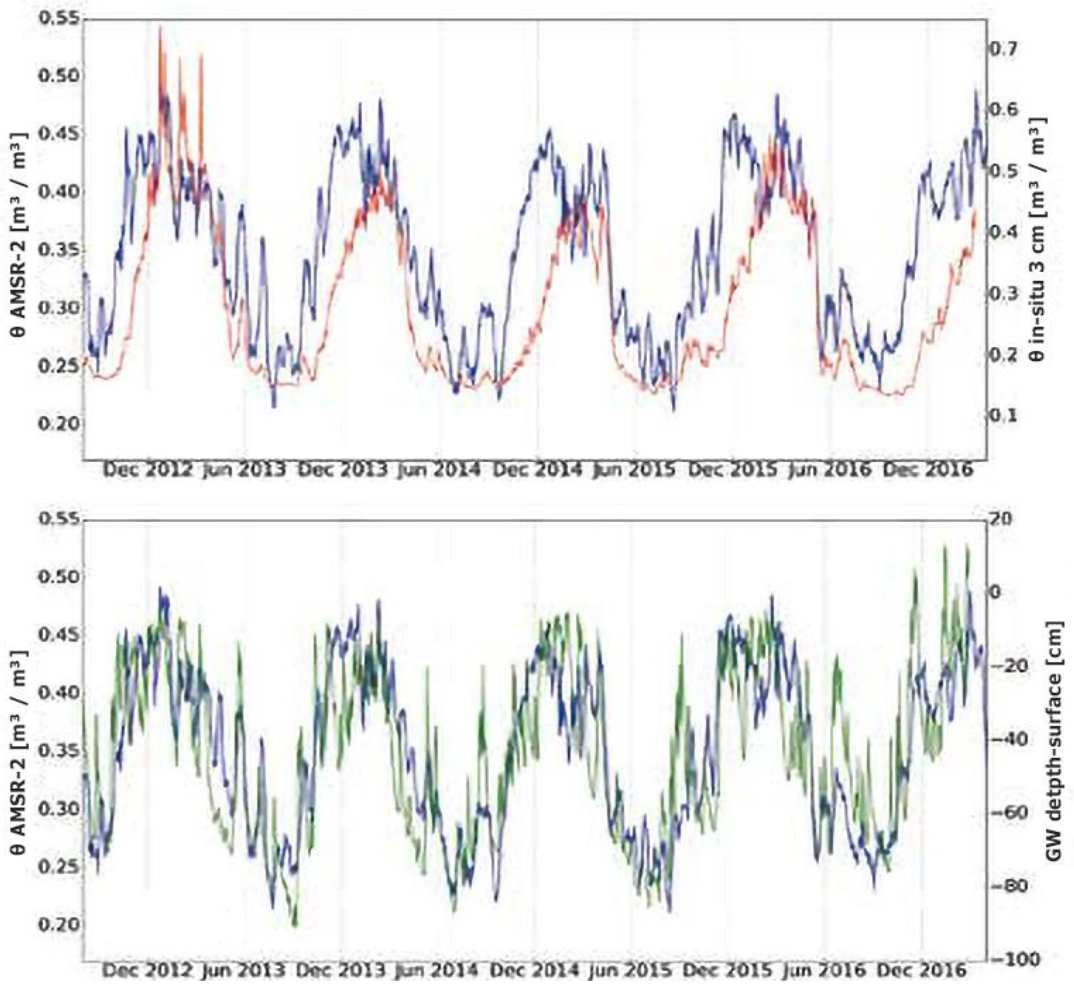

Figure 4.7 Timeseries of VanderSat (AMSR-2) [blue] versus in-situ soil moisture at 3 cm depth [red] and groundwater levels [green] at Cabauw (de Jeu & de Nijs, 2017).

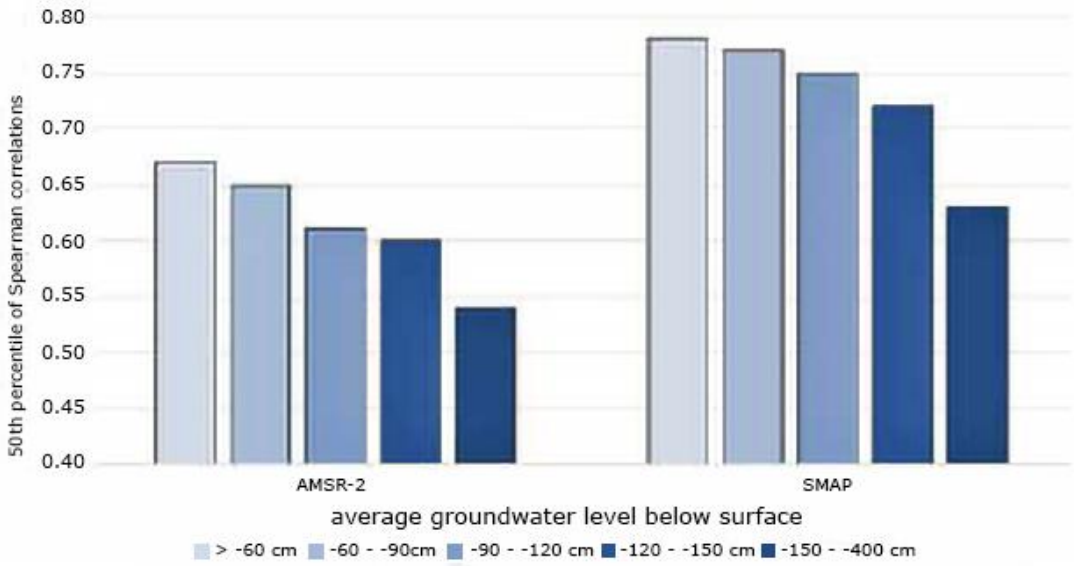

Figure 4.8 Grouped groundwater depths relative to the calculated (50th percentile) Spearman correlations between the groundwater level and the soil moisture products (de Jeu & de Nijs, 2017).

4.2 Correlation of remote sensing products to in-situ measurements

4.2.1 OWASIS

Single cell and 3x3-grid

The results of the *single cell* correlation of OWASIS vs in-situ show that the Pearson correlation (R) ranges from -0.41 to 0.90 over the individual sites, with a mean of 0.32 and a standard deviation of 0.39 (Figure 4.9, left). This means that the degree to which in-situ soil moisture can be 'predicted' by the OWASIS soil moisture product is highly varying from site to site. For the *3x3-grid* correlation of OWASIS vs in-situ the Pearson correlation (R) ranges from -0.25 to 0.80, with a mean of 0.29 and a standard deviation of 0.34 (Figure 4.9, right). The Spearman correlation (ρ) for OWASIS *single cell* ranges from -0.15 to 0.92, with a mean of 0.35 and a standard deviation of 0.33 (Figure 4.10, left). For the *3x3-grid* comparison of OWASIS the Spearman correlation (ρ) ranges from -0.34 to 0.83, with a mean of 0.22 and a standard deviation of 0.37 (Figure 4.10, right).

If we compare the *single cell* version and the *3x3-grid* version, it can be seen that the correlations (both Pearson and Spearman) increased for WSAM_Raam_05, WSBD_Bavel and WSBD_Rijsbergen. The correlations remained (almost) equal for WSAM_Raam_04, 10, 12 and 13. But for most sites the correlations decreased: WSAM_Bult, WSAM_Raam_01, 03, 06, 08, 09, 11, 14, 15. For WSAM_Raam_02 the Pearson correlation became less negative, but the Spearman correlation became more negative. For WSAM_Raam_07 the Pearson correlation changed from negative to slightly positive, but the Spearman correlation remained unchanged.

If the correlations are averaged over all sites, the results show that the Pearson and Spearman correlations perform very similar (Table 4.4).

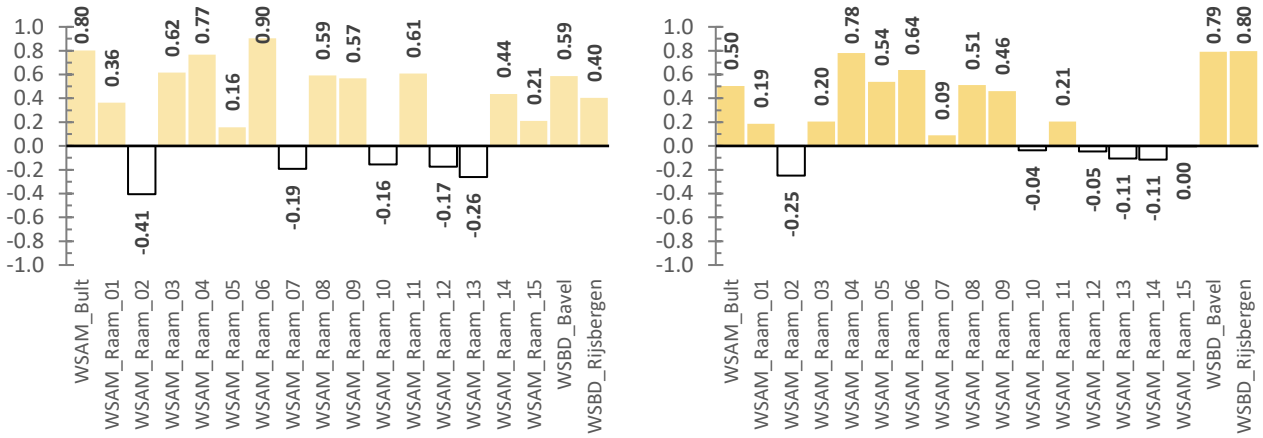

Figure 4.9 Pearson correlation (**R**) of OWASIS vs in-situ (@ 15-20 cm depth). *Single cell* (left) and *3x3-grid* (right).

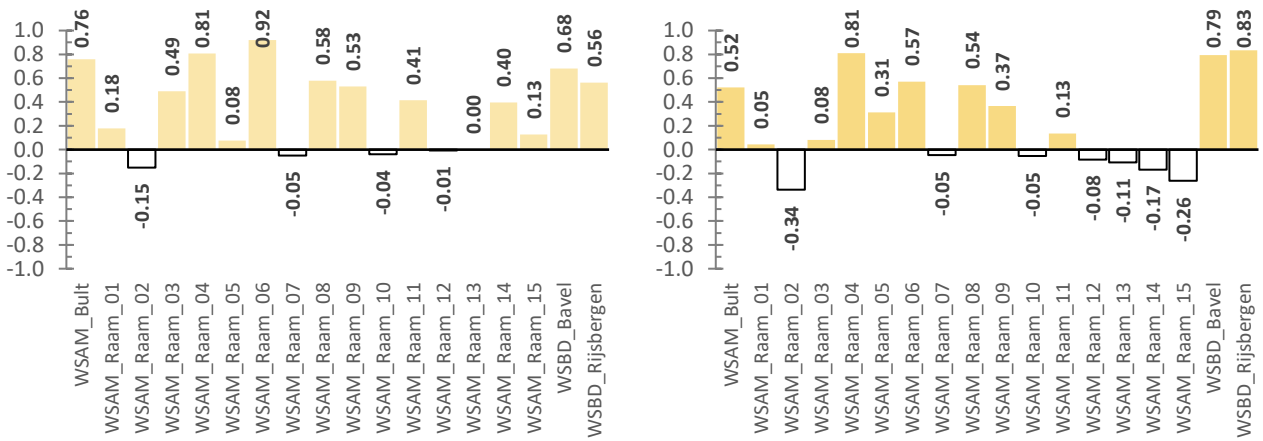

Figure 4.10 Spearman correlation (**ρ**) of OWASIS vs in-situ (@ 15-20 cm depth). *Single cell* (left) and *3x3-grid* (right).

Table 4.4 Overall correlation coefficients for OWASIS vs in-situ (@15-20 cm depth).

OWASIS vs in-situ	**Pearson corr. (R)**				**Spearman corr. (ρ)**			
	Mean	***Std***	***Min***	***Max***	***Mean***	***Std***	***Min***	***Max***
Single cell	0.32	0.39	-0.41	0.90	0.35	0.33	-0.15	0.92
3x3-grid	0.29	0.34	-0.25	0.80	0.22	0.37	-0.34	0.83

Correlation on a calendar month basis

If the correlation results of OWASIS (*3x3 grid*) to in-situ are split out to a calendar month basis (Table 4.5) it can be seen that the values are distributed from as low as -0.6 and up to 0.98. 101 out of 170 (59%) of the individual monthly correlations are strong to very strong ($0.7 \leq R \leq 1.00$). This is also true when all sites are grouped together to produce monthly means (7 out of 12 months). The months June and July show the strongest correlation with 0.88 and 0.89, respectively. The month May shows particularly poor results; for 5 out of 9 sites the correlation was negative (for the other 9 sites a correlation could not be calculated due to a lack of in-situ data). These results show that the OWASIS product performs differently for each location and through time over the year, possibly indicating that the model input data or calculations vary per location and time of the year. In personal communication and in a webinar, HydroLogic noted that this is true because the modeled rootzone is dynamic, which is further explained in the Discussion chapter.

Table 4.5 Correlation of OWASIS (*3x3-grid*) to in-situ measurements on a calender month basis.

NB empty cells represent insignificant correlations and/or missing values

Month	WSBD_Bavel	WSBD_Rijsbergen	WSAM_Raam_01	WSAM_Raam_02	WSAM_Raam_03	WSAM_Raam_04	WSAM_Raam_05	WSAM_Raam_06	WSAM_Raam_07	WSAM_Raam_08	WSAM_Raam_09	WSAM_Raam_10	WSAM_Raam_11	WSAM_Raam_12	WSAM_Raam_13	WSAM_Raam_14	WSAM_Raam_15	WSAM_Bult	Mean	Standard Deviation
January	0.89	0.80	0.84	0.65	0.84	0.86	0.79	0.86	0.65	0.65	0.80	0.78	0.97	0.87	0.86	0.48	0.95	0.71	0.79	0.12
February	0.96	0.98	0.72	0.86	0.52	0.91	0.35	0.80	0.79	0.45	0.95	0.55	0.98	0.37		0.80	0.86	0.64	0.73	0.21
March	0.92	0.46	0.84	0.93	0.82	0.93		0.46	0.71	0.89		0.77	0.97	0.36	0.34	0.78	0.89		0.74	0.21
April	0.71	0.80	0.78	0.45	0.55	0.25	0.63	0.70	0.26	0.28	0.43	0.43	0.36	0.68	0.38	0.63	0.46		0.52	0.18
May				-0.58	-0.25	0.67	0.54	0.26				0.56	-0.41	-0.46	-0.60				-0.03	0.50
June			0.95	0.95	0.95	0.93	0.77	0.97	0.71	0.92	0.93		0.96	0.96	0.84	0.78	0.89		0.89	0.08
July			0.95	0.94	0.93	0.96	0.97	0.98	0.91	0.96	0.92		0.98	0.90	0.95	0.65	0.33		0.88	0.17
August			0.93	0.49	0.77	0.90	0.81	0.96	0.89	0.92			0.96	0.60	0.91	-0.27			0.74	0.34
September			0.69	0.43	0.58	0.84	0.86	0.92	0.53		0.49	0.66	0.92	0.40	0.68		-0.30	0.90	0.61	0.31
October			0.75	0.79	0.88	0.93	0.92	0.85	0.85	0.39	0.66	0.87	0.94	0.43	0.87	0.76	0.85	0.65	0.77	0.16
November			0.33	0.39	0.77	0.84	0.65	0.85	0.82	0.37	0.57	0.72	0.82	0.44	0.71	0.71		0.84	0.65	0.18
December			0.44	0.45	0.31	0.66	0.45	0.71				0.32	0.36		0.47				0.46	0.13
Mean	**0.87**	**0.76**	**0.75**	**0.56**	**0.64**	**0.81**	**0.70**	**0.78**	**0.71**	**0.65**	**0.72**	**0.63**	**0.73**	**0.50**	**0.58**	**0.59**	**0.62**	**0.75**		

Catchment average

Correlations between OWSIS and in-situ were also calculation for the Raam catchment as a whole. This was done at a 7-day moving average (Figure 4.11). Taking the catchment average could potentially mitigate the spatial mismatch in representative area between the soil moisture data product (OWASIS) and the in-situ soil moisture measurements. Because the multiple in-situ sensors are also averaged, any measurement errors (e.g. relatively poor installation, wrong readings) are smoothed out. Applying the 7-day moving average slightly smooths the temporal variation, thus reducing strong changes that occur on a short time scale (e.g. a short peak due to a wrong measurement). This potentially makes the series better comparable, while losing some detail.

The found Pearson and Spearman correlations are very weak, with values of 0.18 and 0.16, respectively (Table 4.6); while the mean correlation of the individual sites was in the order of 0.32-0.35 (Table 4.4). The bias, mean absolute error (MAE) and root-mean-squared-error (RMSE) could not be calculated for OWASIS, because the units did not match with the in-situ measurements (mm and m^3/m^3, respectively).

Table 4.6 Metrics for the relation between OWASIS and in-situ soil moisture (Raam catchment average, 7-day moving average).

Number of paired observations	1038
Pearson correlation (R)	0.18
Spearman correlation (ρ)	0.16

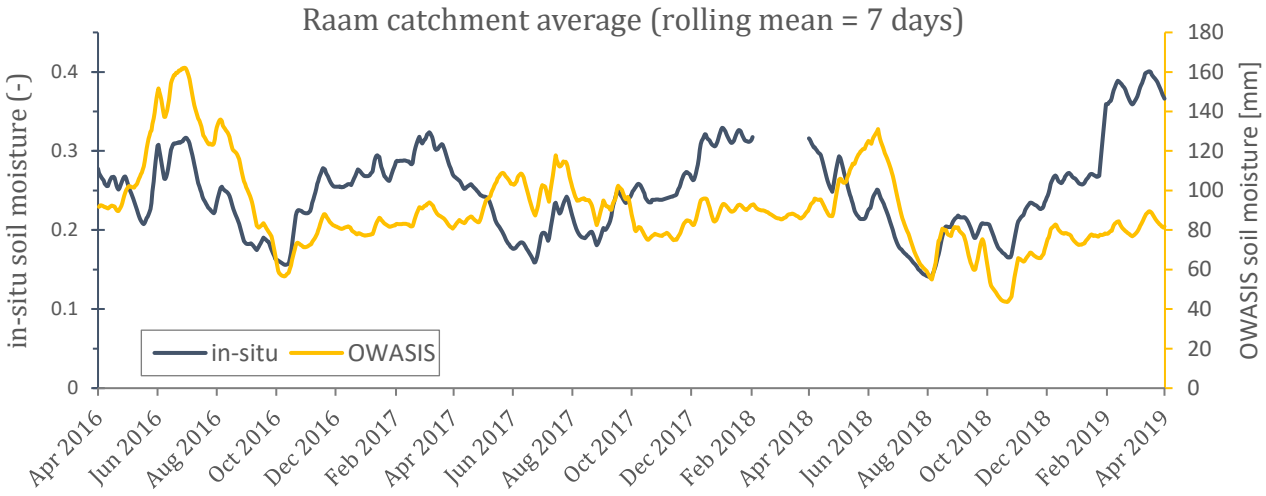

Figure 4.11 Timeseries of Raam catchment-averaged 7-day moving average in-situ and OWASIS soil moisture from April 2016 to April 2019. *NB the two vertical axes represent different units, which may skew perceived trends.*

4.2.2 VanderSat L-band

Single cell

The results of the *single cell* comparison of VanderSat (L-band) vs. in-situ soil moisture show that the Pearson correlation (R) ranges from 0.45 to 0.83, with a mean of 0.66 and a standard deviation of 0.11 (Table 4.7 & Figure 4.12, left). This means that the degree to which in-situ soil moisture can be 'predicted' by the VanderSat soil moisture product in a linear way is 45-83%. The Spearman correlation (ρ) ranges from 0.51 to 0.82, with a mean of 0.69 and a standard deviation of 0.10 (Figure 4.12, right). Furthermore, the bias shows that for 10 out of 15 sites VanderSat slightly overestimates the soil moisture, compared to in-situ measurements. The site WSAM_Raam_09 shows the highest overestimation, with a difference of 0.110 [m³/m³]. The highest underestimation is found at site WSAM_Raam_01, with a difference of -0.070 [m³/m³]. The mean-absolute-error (MAE) of the VanderSat soil moisture product is 0.068 [m³/m³].

A *3x3-grid* correlation was not made for the VanderSat product, because there was no large cell-to-cell variation in this product and thus this extended method was assumed obsolete.

Table 4.7 Metrics for VanderSat vs in-situ (@ 5cm surface) (*single cell*).

Location	Number of observations	Bias	RMSE	MAE	Pearson R	Spearman ρ
WSAM_Bult	-	-	-	-	-	-
WSAM_Raam_01	726	-0.070	0.092	0.078	0.61	0.61
WSAM_Raam_02	672	0.026	0.047	0.038	0.83	0.82
WSAM_Raam_03	720	0.089	0.112	0.092	0.59	0.55
WSAM_Raam_04	727	-0.025	0.049	0.039	0.80	0.78
WSAM_Raam_05	664	0.006	0.049	0.039	0.72	0.72
WSAM_Raam_06	562	-0.033	0.090	0.078	0.53	0.70
WSAM_Raam_07	702	-0.031	0.052	0.042	0.79	0.79
WSAM_Raam_08	524	0.042	0.076	0.061	0.78	0.82
WSAM_Raam_09	471	0.110	0.131	0.117	0.45	0.51
WSAM_Raam_10	602	0.044	0.075	0.063	0.58	0.66
WSAM_Raam_11	687	0.016	0.057	0.045	0.74	0.75
WSAM_Raam_12	678	0.046	0.135	0.120	0.56	0.56
WSAM_Raam_13	672	0.077	0.120	0.104	0.54	0.57
WSAM_Raam_14	708	0.001	0.052	0.040	0.73	0.79
WSAM_Raam_15	724	-0.017	0.072	0.058	0.70	0.73
WSBD_Bavel	-	-	-	-	-	-
WSBD_Rijsbergen	-	-	-	-	-	-
Mean	**656**	**-0.019**	**0.081**	**0.068**	**0.66**	**0.69**
Standard deviation	**77**	**0.049**	**0.030**	**0.028**	**0.11**	**0.10**
Min	471	-0.110	0.047	0.038	0.45	0.51
Max	727	0.070	0.135	0.120	0.83	0.82

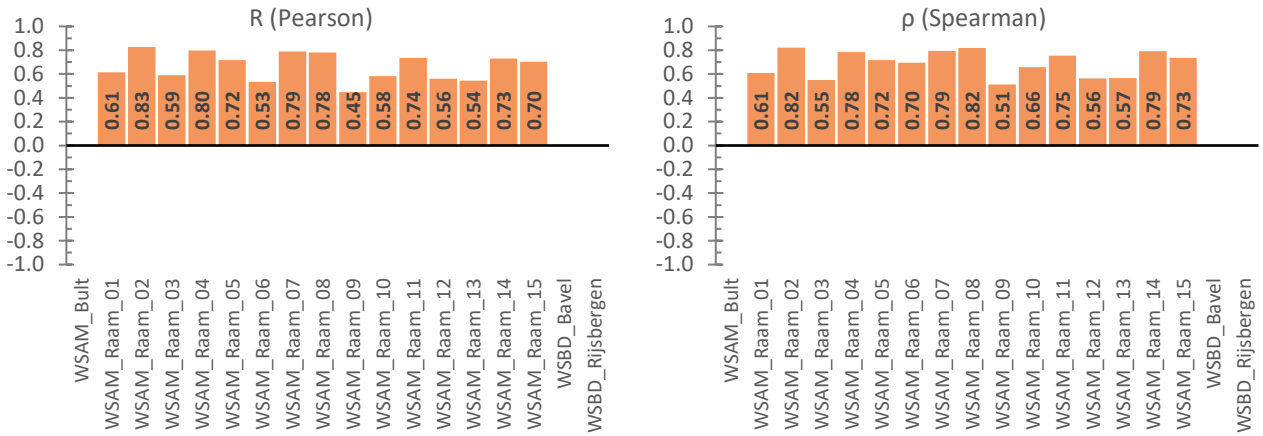

Figure 4.12 [**left**] Pearson correlation (**R**) of VanderSat L-band vs in-situ (5 cm-surface). [**right**] Spearman correlation (**ρ**) of VanderSat L-band vs in-situ (5 cm-surface).

Due to the more promising results compared to OWASIS, the VanderSat product was further analyzed in terms of spatial distribution. The Pearson correlations were geographically plotted on a map of the Raam catchment area (Figure 4.13). Some weak clusters of similar correlation are apparent (e.g. WSAM_Raam_09,10,12,13 and WSAM_Raam_07,14,15). Contrary, there are also clusters of mixed high and low correlations (e.g. WSAM_Raam_01 trough 06,15) Therefore, it may be assumed that there is no noticeable trend in the spatial distribution.

Figure 4.14 shows the separate timeseries for the in-situ measurements (top panel) and the VanderSat soil moisture product (bottom panel). It can be seen that the in-situ measurements in the top panel have a very high spatial and temporal variation, when compared to the much more gradual and similar timeseries of VanderSat in the bottom panel). In the VanderSat panel, all 15 sites largely follow the same pattern, while the 15 sites show very different patterns amongst each for the in-situ measurements. This might partly be attributed to errors in the in-situ measurements because there are some sites that show soil moisture values less than 0.05 [m³/m³] and over 0.4 [m³/m³]. Such low values are not impossible but are rare due to the fact that some water will always be retained in the pores due to suction, and the high values are rare for sandy soils due to gravity draining the excess water (Figure 2.3). However, it seems more likely that the VanderSat product provides relatively smooth spatial estimates. Literature also indicates that soil moisture can show very high spatial variability (Wang & Qu, 2009), which is not found in the VanderSat product.

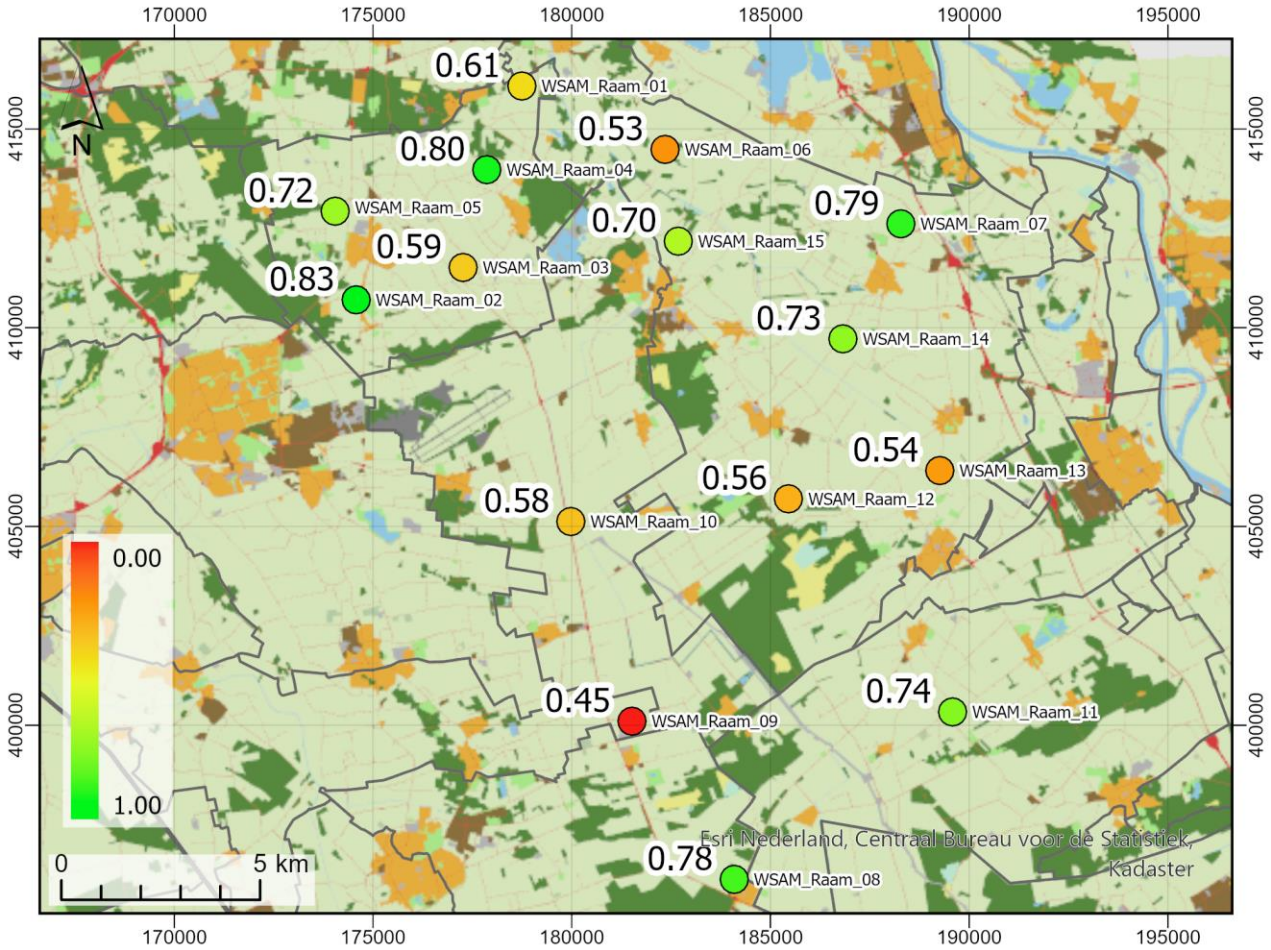

Figure 4.13 Spatial distribution of the Pearson correlation (R) of VanderSat vs in-situ (5 cm-surface) for the Raam sites.

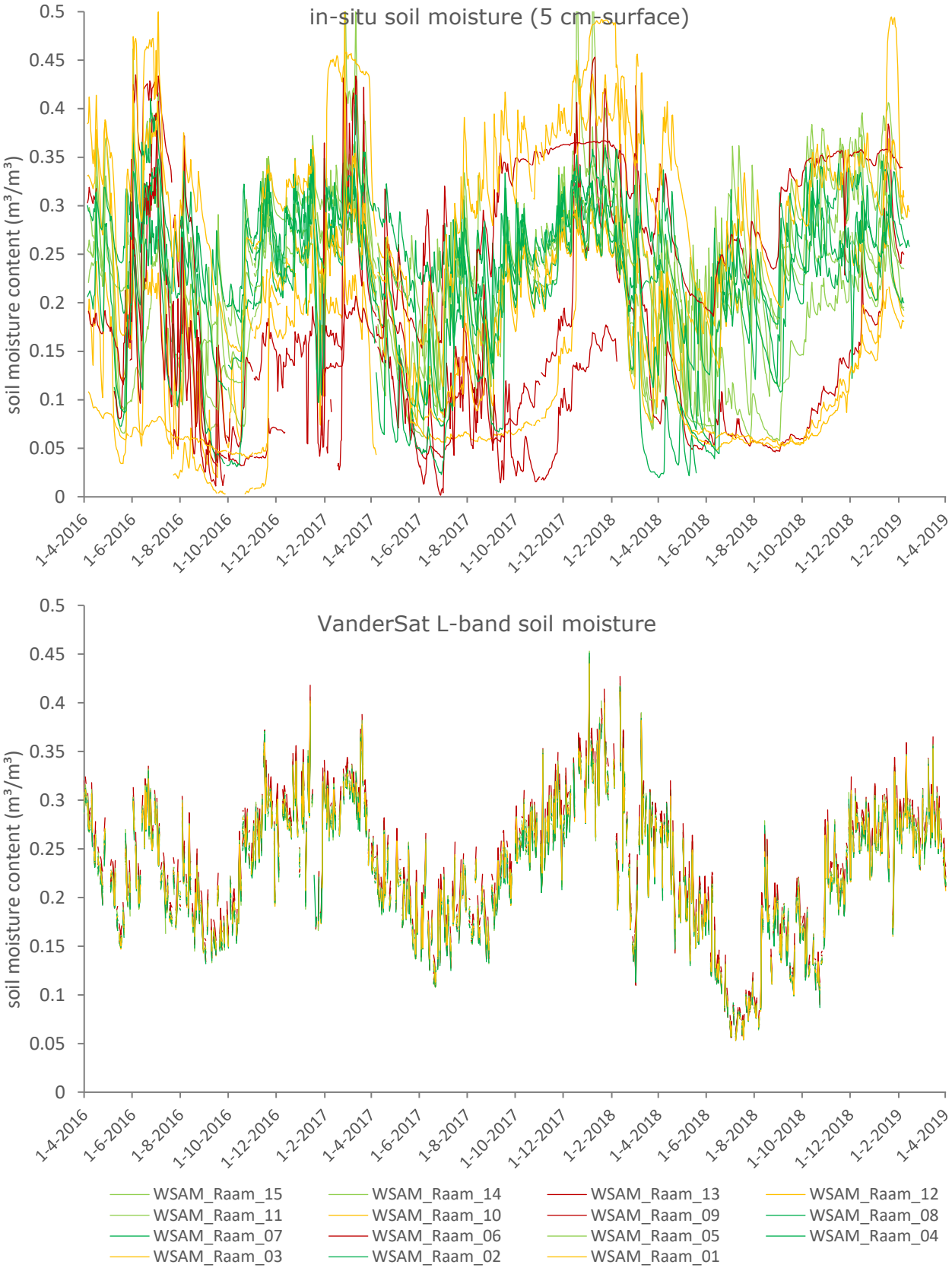

Figure 4.14 **[top]** Timeseries of in-situ soil moisture measurements (5 cm-surface). **[bottom]** Timeseries of VanderSat L-band soil moisture measurements. Individual series are color-coded based on the Pearson correlation between in-situ and VanderSat for that site: red: R=0.45-0.55, orange: 0.55-0.65, light green: 0.65-0.75, dark green: 0.75-0.85. i.e. red timeseries show sites with a relatively poor correlation, while green shows relatively good correlations.

Catchment average

Similar to OWASIS, an analysis for the Raam catchment as a whole was made for VanderSat, at a 7-day moving average to mitigate the mismatch in representative area between VanderSat (100 m²) and in-situ data (<1 m²) (Figure 4.15). The obtained Pearson and Spearman correlations were 0.82 and 0.83, respectively (Table 4.8). Overall, the VanderSat L-band product slightly overestimated the in-situ soil moisture, with a bias of 0.008 $m^3\ m^{-3}$, which is on the low end compared to the values found for the individual sites in Table 4.7 (between -0.110 and 0.070, with a mean of -0.019 [m³/m³]). The mean-absolute-error (MAE) for the catchment-average is 0.031 [m³/m³], which is also an improvement over the individual sites (which showed a mean of 0.068 [m³/m³]). In fact, the catchment-average MAE is even smaller than the best-performing individual site, which was WSAM_Raam_02 with a MAE of 0.038.

When looking at the details of the time series (Figure 4.15), it can be seen that during the autumn and early winter of 2016-2017 the soil moisture was overestimated by the VanderSat product by approximately 0.05 [m³/m³]. During the autumn of 2017 the VanderSat product also slightly overestimated the soil moisture, but less noticeable than the previous year. There was no noticeable overestimation for the autumn of 2018. During spring 2018 there seems to be relatively much jitter in the VanderSat product, but no comparison could be made, because no in-situ data was available for that time period. Over the summer of 2018 soil moisture was somewhat underestimated by the VanderSat product. No underestimation was found for the summers of 2016 or 2017. These periods of over- and underestimation were compared to minimum temperatures at 10 cm above surface level, and to daily average temperatures, at KNMI station Volkel (Figure 4.16). Presence of frozen conditions could not explain the difference in measured soil moisture during the winter of 2016, because 2017 and 2018 had mostly similar temperature trends, and there was a freezing period in 2017 which lasted longer than that of 2016.

Table 4.8 Metrics for the relation between VanderSat L-band and in-situ soil moisture (Raam catchment average, 7-day moving average).

Number of paired observations	964
Bias	0.008 [$m^3\ m^{-3}$]
RMSE	0.039 [$m^3\ m^{-3}$]
MAE	0.031 [$m^3\ m^{-3}$]
Pearson correlation (R)	0.82
Spearman correlation (ρ)	0.83

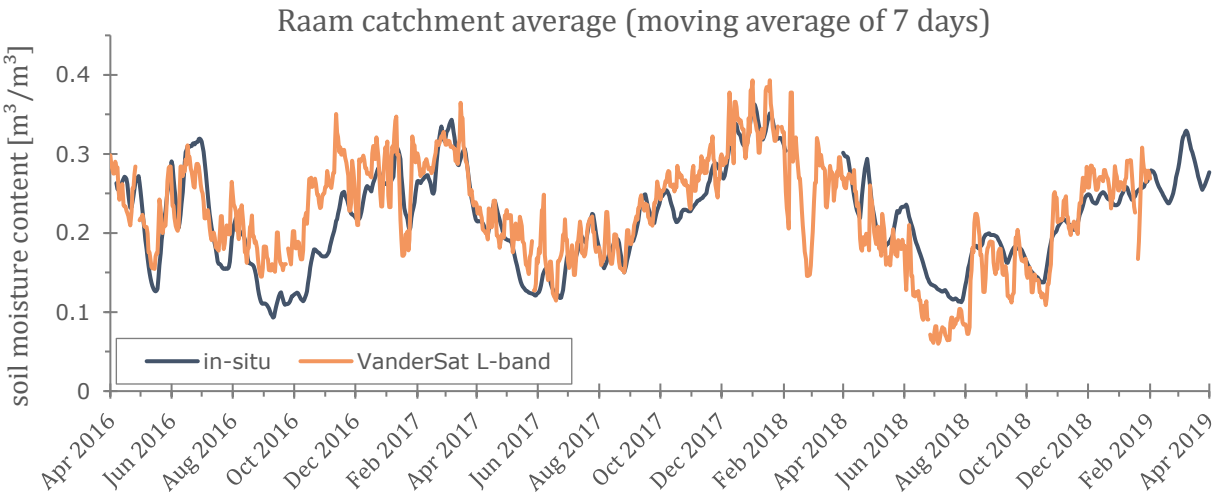

Figure 4.15 Timeseries of catchment-averaged 7-day moving average in-situ and VanderSat L-band soil moisture from April 2016 to April 2019.

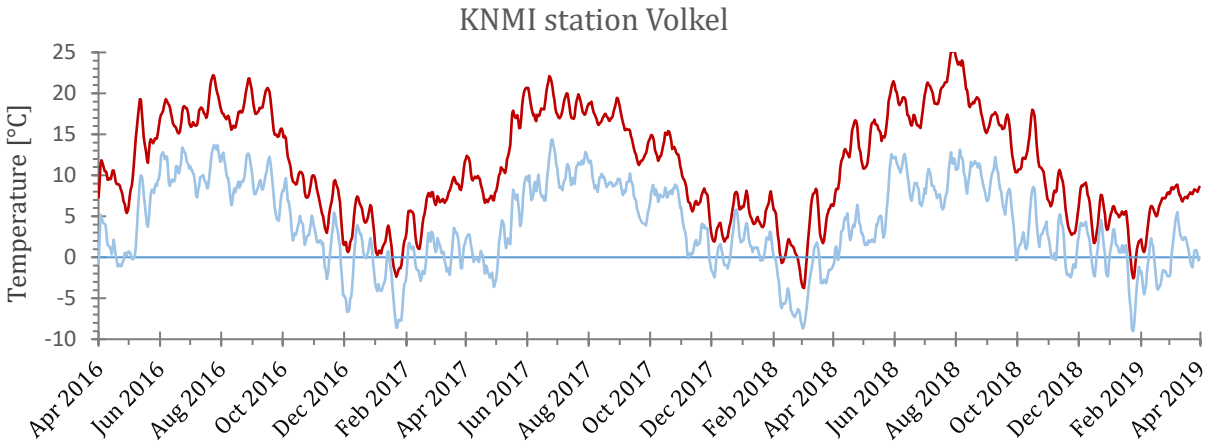

Figure 4.16 Time series from April 2016 through April 2019 of daily mean temperature [**red**] and daily minimum temperature at 10 cm above surface level [**blue**] (at a 7-day moving average) for KNMI station Volkel (source: KNMI).

4.2.3 Linking correlation to soil type, groundwater levels & land-use type

Further explanation for the differences in the correlation between sites was sought in site properties such as soil type, groundwater depths and land-use type. A comparison was made between each site its Pearson correlation and the local soil type (BOFEK2012), groundwater level classification, and basic land-use type. Due to the relatively limited number of sites (between 15 and 18) in relation to the relatively large number of classes (9 soil types, 8 groundwater classes, 2 land-use types) the results turned out to be relatively weak. Therefore, the tables that show the soil type classification, groundwater classification, land-use type and corresponding correlations per site are only provided in Appendix C. The following paragraph is a generalized summary of those results.

In terms of soil type, the classification was made based on the BOFEK2012 dataset. BOFEK2012 is a national map of soil type classifications in the Netherlands (Wosten *et al.,* 2013). There was little variation between the sites, as all had a mainly sandy soil. Slight variations included loamy components (for many sites) or cultivated components (for a few sites). There were 5 very low correlations (< 0.4) for class 304 (loamy sand) for OWASIS. With 5 out of 18 sites, it would seem that the OWASIS product performs particularly poor for that soil type, but the fact is that 7 out of the 18 sites are of class 304. That class is therefore overrepresented in the dataset (in other words, the number of sites per soil unit is not equally distributed). The VanderSat product showed better correlations for that class (1 site between 0.4-0.5, 3 sites between 0.5-0.6, 2 sites between 0.7-0.8), which may indicate that the poor correlations for OWASIS are more likely to be related to model performance, rather than the local soil type.

Groundwater levels were classified based on the Dutch system of '*grondwatertrappen*'. That system has a number of classes that are expressed in Roman numerals and that represent specific ranges of the absolute groundwater level and its fluctuation. The classes are defined on the basis of the average highest groundwater level (GHG) and average lowest groundwater level (GLG). Most of the sites were classified as VI or VII, which coincides with a GHG of 40-80 cm or >80 cm, respectively, and a GLG of >120 cm in both classes. Classes III, IV, V (shallower GW) and VIII (deeper GW) each contained one site. For groundwater class VI most sites (7 out of 9) had a correlation ≤ 0.6. For class VII 4 out of 5 sites had a correlation ≤ 0.6. Again, the distribution of sites between classes is too poor to say that these two particular groundwater classes lead to poor correlations.

Land-use type was classified as grassland or agricultural land. The sites were classified based on optical satellite imagery from www.satellietdataportaal.nl over the years 2016-2019. For some sites no distinction could be made based on optical imagery (e.g. seasonal variation), those were marked as both grassland and agricultural. For the sites WSAM_Raam_02, 03, 05, 14, photographs were available from the time of sensor installation. These photographs were used to verify the land-use type for those sites. From these photographs it also became clear that for some fields the land-use was agricultural (based on satellite imagery), but the sensor was placed at the very edge, which consisted of a patch of grass(land). One should take this into account when judging the results. The results (Table 4.9) showed similar correlations for

agricultural land and grassland, for both OWASIS and VanderSat. Thus, likely because the sensors were all placed at the edges of fields (often in a patch of grass).

Table 4.9 Averaged Pearson correlation (R) per land-use type.

	Agricultural field	**Grassland**
OWASIS *3x3 grid*	0.18	0.19
VanderSat *single cell*	0.68	0.67

4.3 Relation between precipitation, soil moisture and discharge

The relations between daily precipitation, soil moisture state, groundwater level and daily discharge are visually laid out as a scatterplot with three classes of color coding (Figure 4.17). The color indicates the states of the soil moisture (in panel a) and the groundwater depth (panel b): red for relatively dry conditions and blue for relatively wet conditions.

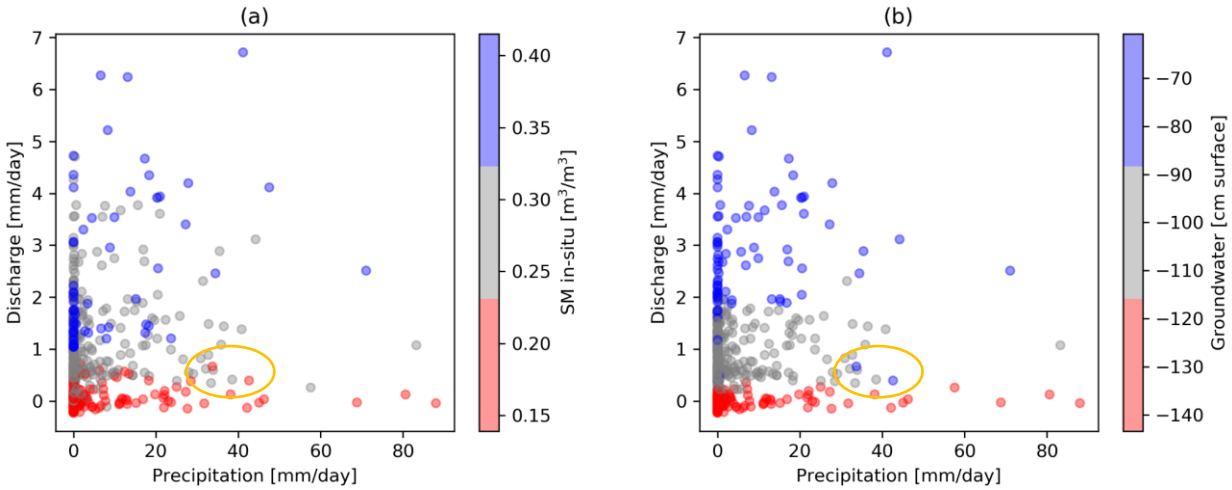

Figure 4.17 Scatterplots of precipitation and discharge. **[a]** Color coding based on soil moisture state. **[b]** Color coding based on groundwater depth below surface level.

The results show that most events are located in the bottom-left corner. These are common events of low precipitation intensity ~0-20 mm/day), resulting in low discharge (~0-1 mm/day). In panel (a) of Figure 4.20, it can be seen that on days were soil moisture was relatively low (red markers), the coinciding discharge was also low (<1 mm/day), regardless of precipitation intensity. Even under rare events of 70-90 mm of precipitation on a single day the discharge remained low, if soil moisture was low. On two other days were precipitation intensity was 60-80 mm/day the soil moisture states were medium and high, which resulted in higher discharges compared to the dry conditions. More extreme cases of high discharge under wet conditions can be found in the top-left of the plot. In those cases, precipitation of less than 20 [mm/day] resulted in discharges in excess of 6 mm/day.

The far left of the plot shows many days without precipitation, while the discharge still varied between 0 and 5 [mm/day]. This may possibly be due to baseflow, e.g. water originating from an area that was not considered in the analyses, or from delays, as it takes time for the water to drain through the soil and into the surface water after a precipitation event. Regardless, low soil moisture conditions generally still result in low discharges. The medium to high soil moisture conditions show a somewhat more mixed pattern, but generally the wet conditions results in higher discharges.

Panel (b) of Figure 4.17 shows generally the same story as panel (a), in the sense that low groundwater levels (= dry conditions) result in low discharge, regardless of precipitation intensity. Different from the soil moisture conditions, almost all wet conditions in terms of groundwater levels (blue markers) now result in higher discharge than the average conditions (grey markers). In other words, the points are now clearly divided between dry, average, and wet conditions. The fact that the dry and average conditions show a somewhat mixed pattern in panel (a) and not in panel (b), indicate that the amount of discharge resulting from precipitation, mainly depends on the groundwater depth and to a lesser extent depend on soil moisture state. However, it can also be seen that this is not a rule written in stone, as examples are present that show the opposite. Two obvious outliers are present in panel (b): events of ~35-40 mm of precipitation on a single day with high groundwater levels, while still resulting in a low discharge of <1 mm/day (orange circle). This may be explained by the fact that, although groundwater levels were high, the soil moisture conditions were dry, as can be seen in panel (a). This shows that cases exist were the soil moisture content appears to be more important than only the groundwater depth. Worth noting is that the two outlier events were only 3 days apart, 29-05-2018 and 01-06-2018 (Table 4.10). Thus, they were strongly coupled in

terms of the hydrologic conditions, rather than being two completely different events. The current research provides no answer to what made these particular events different from the rest of the dataset. Extending the dataset with weir elevation data may help explain which part of the hydrologic conditions is due to natural processes and which part is due to water management.

Table 4.10 Part of the P, Q, SM, GW dataset between 23-05-2018 and 08-06-2018. The events that are indicated with the orange circle in Figure 4.17 are shown here in yellow.

Date	Precipitation [mm/day]	Discharge [mm/day]	SM in-situ [m³/m³]	Groundwater depth [cm surface]
23-05-2018	13.4	0.5	0.221	-106.079
24-05-2018	2.8	0.5	0.219	-106.45
25-05-2018	0.0	0.5	0.22	-107.2
26-05-2018	0	0.4	0.21	-108.3
27-05-2018	18.3	0.4	0.21	-97.9
28-05-2018	0.1	0.4	0.21	-78.1
29-05-2018	**42.6**	**0.4**	**0.21**	**-80.4**
30-05-2018	0.0	0.4	0.22	-76.3
31-05-2018	0.4	0.5	0.22	-79.0
01-06-2018	**33.7**	**0.7**	**0.22**	**-83.8**
02-06-2018	0.1	0.8	0.22	-85.3
03-06-2018	0	0.6	0.23	-89.0
04-06-2018	0	0.4	0.24	-91.7
05-06-2018	0	0.3	0.23	-94.0
06-06-2018	0	0.4	0.23	-96.3
07-06-2018	2.6	0.1	0.22	-98.2
08-06-2018	83.3	1.1	0.25	-91.7

5 Discussion

Soil moisture content is a variable that is often not measured with high spatial coverage, this has also become clear in the research from the fact that the WSBD area has only two measurement sites, as of begin 2020. Therefore, it was especially helpful that WSAM data from over 15 soil moisture sensors could be used, which was also relatively evenly distributed over a single catchment. Although 15 sites may still be low for very detailed analyses, it has offered much better results compared to only 2 sensors in the WSBD area. Furthermore, the WSAM data spanned multiple years (2016-2019), this helps to filter out biases that may be present during extremely dry or wet years.

In the correlation analysis, moderate results were obtained for the VanderSat L-band soil moisture product at *single cell* scale (site-averaged R=0.66). Good results were obtained for this product at catchment scale (R=0.82). The mean absolute error for VanderSat compared to in-situ measurements was 0.068 [m³/m³] (*single cell*) and 0.031 [m³/m³] (at *catchment scale*). References for comparing the accuracy are not readily available, but we may compare to the target accuracies of soil moisture satellites (SMAP and AMSR2), which were set at 0.04 [m³/m³] (Ye *et al*, 2019). Those relate to the RMSE, which in the research were 0.081 [m³/m³] (*single cell*) and 0.039 [m³/m³] (at *catchment scale*). The required release accuracy for AMSR2 SMC products is ±0.1 [m³/ m³], while the desired goal accuracy is ±0.05 [m³/m³] (Wu *et al*, 2016). If these accuracies are used as a reference, this indicates that the performance of the VanderSat product is sufficient to accurately predict (top)soil moisture content at catchment-average scale but is likely insufficient at very local scale. For inundation risk assessment this may be considered sufficient, as this is generally done at (sub)catchment scale rather than at the scale of individual ditches or parcels.

The results that were found for the WSAM area are considered generally applicable (or scalable) to the WSBD area as well, due to the largely similar conditions: The WSAM area is geographically not very far from WSBD, implying no major differences in meteorological forcing. The general soil type is comparable (sandy soil). The surface heights compared to N.A.P. may be up to a few meters higher at WSAM, but no exceptionally large differences are present.

5.1 Quality of the research methods

The accuracy of the results is subject to the quality of the used data and the applied methods of analysis.

In-situ measurements

All correlation analyses rely on the in-situ measurements. It should be kept in mind that, although used as a reference in this research, those measurements cannot be considered as 100% accurate. This is because any sensor instrument has limitations to its capabilities in terms of measurement accuracy and resolution. If we assume that installation was done properly, meaning good (undisturbed) soil contact around the sensor, the sensor accuracy would normally introduce a maximum error of ±0.02-0.03 m^3/m^3 (2-3%) (Table 3.2; Benninga *et al*, 2018). Furthermore, an in-situ sensor represents a soil volume of <500 mL, which equals an area of only a few centimeters around the sensor and which may not be representative for the spatial scale at which remote sensing products operate. Remote sensing products are made up of area-averaged data at hectometer scale. Soil properties can have strong variation due to local hydrological conditions, especially in the shallow subsurface, e.g. local macro pores that can strongly determine the soil water conditions. Due to this large variability in soil moisture, it is difficult to directly relate point measurements to remote sensing observations (Western and Blöschl, 1999).

It should also be considered that estimation of soil moisture for the full unsaturated zone may be difficult based on near-surface soil moisture (as obtained from remote sensing). Mahmood and Hubbard (2007) noted that there is a tendency to equate near-surface soil moisture to the whole root zone (or unsaturated zone), however their results and other studies (Santanello and Carlson, 2001) showed that this assumption is not justified. This is important for the research in terms of inundation risk, because in that case the

estimated value from remote sensing does not relate to the full unsaturated zone. Making the conversion from near-surface to the full unsaturated zone would require a model calculation (with associated uncertainties).

Difference in correlation between single cell, 3x3-grid, and catchment average

Single cells in OWASIS have shown high variability to their neighboring cells in multiple cases, possibly explained by differences in rootzone depth or other input parameters. Regardless, if it were the case that (by error) the OWASIS cell does not match the in-situ sensor, the resulting correlation may be very different. Averaging over 3x3 cells in OWASIS shows different results. The results showed that for some sites the correlation improved, but for most it decreased or remained equal. This means that if the data of the single cell was poorly matching the in-situ sensor by error, then averaging over multiple cells could improve the correlation. But in the case that the single cell already correctly matched the in-situ sensor, the correlation would likely decrease due to the smoothing that occurs when adding extra cells. Therefore, if this method is applied (e.g. in future research), averaging should be considered per site, rather than doing it for all.

Taking the catchment average (for the Raam) theoretically had good potential to minimize errors due to local variability. For the VanderSat product this worked relatively well, with a correlation of R=0.82 and a MAE in volumetric moisture content of 0.031 [$m^3\ m^{-3}$]. However, for OWASIS the results turned out very poor, with a correlation of R=0.18. To further improve the accuracy of this method, one could increase the number of in-situ sensors (and spatially distribute these evenly over the catchment). This helps because the spatial catchment average of the remote sensing products is based on ~1000-2000 individual cells (for OWASIS) and ~10.000 cells (for VanderSat), while there were only ~12-15 in-situ sensors in the Raam catchment. If it were the case that multiple remote sensing cells were erroneous, the (remotely sensed) catchment-average soil moisture value would remain roughly equal. While, if only one sensor is erroneous, the in-situ average may shift considerably.

Limitations in OWASIS

From the beginning of 2016 until 31-12-2019, the OWASIS model used the *eLEAF evaporation* product as input. For the first half of 2020 the OWASIS model was undergoing a transition to a new evaporation data service. As a consequence, OWASIS temporarily used reference evapotranspiration, rather than the remote sensing actual evapotranspiration (HydroLogic, personal communication). This implies that data that was used for 2020 may not be representative for the OWASIS product as it should be (i.e. using remote sensing ET_{act}). This problem only applies to the WSBD sites (7-1-2020 – 22-4-2020), because for all other sites data from 2020 was not included.

Furthermore, from observations early in the research, it turned out that for multiple sites there was a relatively large spatial variation between neighboring cells, of up to one order of magnitude (e.g. ~50 mm of soil moisture in one cell and >150 mm in the next). Even though this can possibly be explained by the spatially variable nature of soil moisture, doubts arose whether this was caused by the OWASIS model. In addition, there were sometimes very strong jumps in soil moisture values (Figure 5.1), which seemed to coincide with the agricultural crop season. From personal communication with HydroLogic, it was identified that the OWASIS model provides the soil moisture value for the rootzone, rather than the full unsaturated zone. The extent of the rootzone could vary spatially and temporally, based on mapped soil type, vegetation type, and stage of the crop growth season. A HydroLogic validation report showed that the modelled rootzone varied between 0.25 m and 1 m throughout the Raam sites in 2016. However, for the current research it was not possible to retrieve the modelled rootzone depth over time and space. This has large consequences for the usability of the data, because not knowing the total depth of the rootzone, makes it impossible to convert the data to a volumetric fraction (e.g. m^3/m^3). In the current situation it is unclear what the data is representing through time and space. As a consequence, the values can actually not properly be compared to in-situ measurements.

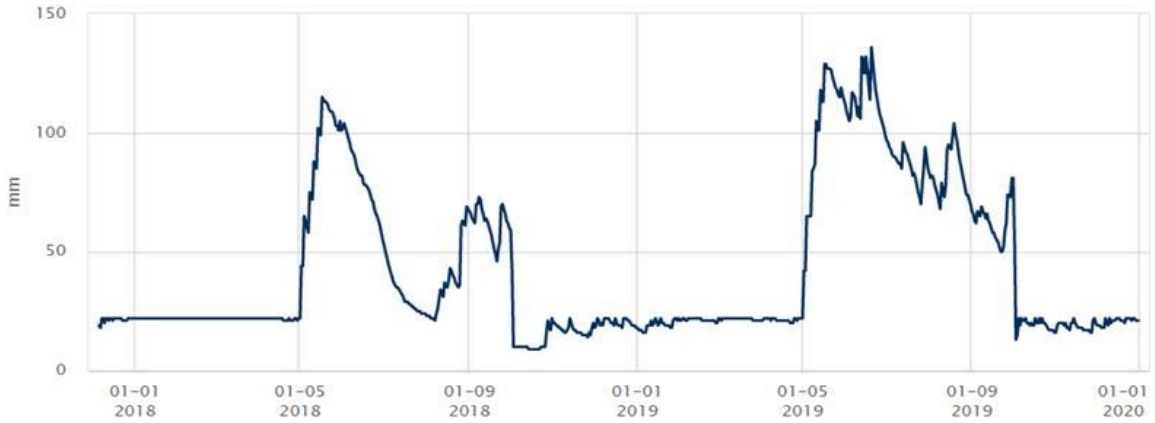

Figure 5.1 OWASIS timeseries showing an example of large seasonal jumps in soil moisture value (source: HydroNet).

Limitations in VanderSat

Although the VanderSat product is supposed to be updated on a daily basis, roughly 3 out of every 10 days there was a missing value in the dataset. The primary cause seems to be the orbit of the (SMAP) satellite, e.g. no overpass on specific days, as there is a periodic trend in the data, where one cycle generally consists of two consecutive measurements followed by a missing value, then four measurements followed by a missing value. There were also cases of extra missing values, which were likely caused by one of the circumstances that VanderSat incorporates in their data flags (e.g. frozen soil, snow or severe rainfall, high vegetation, radio frequency interference, instrumental flaws or the value being out of the valid range). Under those conditions, the measurement is omitted. For the research, these missing values affected the calculation of the 7-day moving average. The applied calculation method ignored the missing values and used only the values that were present in the applicable time frame, e.g. only 6 out of 7 values.

As could be seen in the timeseries of the individual sites (Figure 4.14, bottom panel), there is very little spatial variation in the VanderSat product. Sites that were up to 20 km apart showed virtually the same soil moisture values. The spatial variation among simultaneous in-situ data was much larger. This indicates that the VanderSat soil moisture does not correctly match the in-situ state.

Time of measurement during the day

The in-situ soil moisture and remote sensing soil moisture are both provided on a daily basis in the research. However, there is a fundamental difference between the two. The in-situ soil moisture measurements are the average value over the full 24 hours of a day, while the remote sensing measurements are instantaneous measurements at a single moment in time. One could expect that the average value over a full day is lower than at the moment during the night, due to the fact that soil moisture evaporation is greater during daytime. A review of the dataset indicated that at 5 cm depth there was generally a difference of ≤0.01 [m^3/m^3] between the soil moisture value at 02:00 h and the daily average, even during mid-summer (July-August). The difference declined with increasing depth. Therefore, it is assumed that this effect has not led to significant errors in the correlation between the in-situ and remote sensing products.

Limitations in the rainfall-runoff analysis

The rainfall-runoff analysis was relatively simplistic in nature, due to the fact that precipitation and discharge (as well as soil moisture conditions and groundwater depth) were directly related to each other without taking into account any (hydrological) processes that occur between the two. For example, evapotranspiration is not considered, thus it is assumed that all precipitation is converted into runoff. Also, storage processes in the subsoil are not considered, meaning that it is assumed that precipitation is instantaneously converted into runoff, while in reality part of the water that is added to the subsoil may reside there for longer periods. This means that from a single rainfall event not all water directly returns in the subsequent discharge peak, and also that a single discharge peak may contain water from earlier rainfall events.

The initial idea for the rainfall-runoff study was to use the WALRUS (Wageningen Lowland Runoff Simulator) model which includes the processes between rainfall and runoff. However, the use of this model failed because the state of the soil moisture could only be input as an initial value and in terms of the storage deficit (i.e. the amount of water that can still be stored in the vadose zone). The subsequent course of the

soil moisture would then be calculated by the model based on water balance formulas. In order to properly do so, it would be required to also input accurate data of many other parameters, including groundwater levels, surface water levels, and catchment parameters (e.g. vadose zone relaxation time, groundwater reservoir capacity, channel depth, a stage-discharge relationship, etc.). This data was not readily available. An attempt was made to estimate some of the parameters by means of calibration and to use default values for less significant general parameters, but this did not lead to sufficient model performance for further research.

5.2 Recommendations to the water authority

In essence we (i.e. the water authority or in general) would like to use these products to up-scale in-situ measurements to catchment scale, but for that specific purpose these products currently give little confidence. This is because the OWASIS soil moisture product is not consistent with the depth of the root zone over time and space, rendering the data unusable for the intended purpose. OWASIS seems to be aimed at agricultural purposes, for which the root zone is very important, rather than water management purposes. The VanderSat product is more consistent because it measures a relatively constant depth of the top layer of the soil. Due to this exact same reason, the value may also not be representative for the entire unsaturated zone. Furthermore, the VanderSat product shows very little spatial variation in the measured values, as could be seen when comparing the 15 individual sites of the Raam catchment. These sites were approximately 1 to 20 km apart, yet the VanderSat product provided soil moisture values that were virtually the same at every site. Contrary, the in-situ data showed much more spatial variability. This smooth nature makes the product much less suitable for up-scaling field measurements to larger areas.

This implies that (1) the *OWASIS soil moisture* product, as currently used in the research, is not reliable enough to draw good conclusions, there are too many unspecified and changing variables in the model for proper application. This may be improved by using *OWASIS available storage capacity* (not shown in this research), which models the remaining available water storing capacity of the full unsaturated zone, rather than available soil moisture in only the rootzone. (2) Based on the obtained correlations, the VanderSat L-band soil moisture product seems reliable enough to be used at the scale of a small catchment (R=0.82), as complementary data to in-situ measurements. In that case, the error in estimated versus in-situ measured volumetric moisture content should be expected to be 0.031 - 0.039 m^3/m^3 (MAE – RMSE). If the product is used at less than catchment scale (e.g. single cell scale of 100 m), the correlation of VanderSat to in-situ is more variable; the lowest correlation found was R=0.45, while the highest was R=0.83. On average R was equal to 0.66. The minimum error was 0.038 – 0.047 m^3/m^3 (MAE – RMSE), while the maximum error was 0.120 – 0.135 m^3/m^3 (MAE – RMSE). In other words, even the lowest error at cell scale is higher than the error at catchment scale. Furthermore, high errors of for example >0.1 m^3/m^3 make the use at cell scale highly unreliable due to the fact that the (in-situ) soil moisture content in the study area generally only varies by ~0.3 m^3/m^3. Finally, the VanderSat product showed very little spatial variation between local sites, making it unuseful for interpolating field measurements.

The rainfall-runoff analysis has shown that groundwater depth generally seems to be the most important factor that determines how precipitation is converted to discharge. High groundwater levels generally led to higher discharges. However, in uncommon cases the groundwater level was relatively high, but the soil moisture content in the top layer was low enough to still accommodate the precipitation, leading to lower discharge compared to the common cases. Thus, for most of the time, these soil moisture measurements may not add significant value to near-future inundation risk assessment, and the assessment can be largely based on groundwater levels. However, the water authority would have to consider whether gaining some additional information under uncommon cases is worth the investment in time and cost.

5.3 Future research

OWASIS available soil storage capacity

In OWASIS there is also a product that estimates the available water storing capacity of the soil (*OWASIS bodemberging*). OWASIS *bodemberging* considers the full unsaturated zone, meaning it could potentially be used as an alternative to the OWASIS soil moisture product which suffers from the dynamic rootzone. The available storage capacity could be converted to soil moisture content if the extent of the unsaturated zone and the porosity are known.

Downscaling remote sensing data variability to in-situ scale

The soil moisture variation of the sensors is likely greater than that of the remote sensing products, because the remote sensing data captures the average value over a larger surface area than an in-situ site. One could compensate for this by calculating the variability of the remote sensing product over an area that is representative for the in-situ measurements. This may be accomplished by calculating the variability over different surface areas (e.g. 1 grid cell, 9 grid cells and 25 grid cells). After plotting the obtained standard deviation for each case against representative surface area, it becomes possible to extrapolate to a smaller (indicative) surface area, representativity of an in-situ sensor (<1 m²) (Figure 5.2). This way we can approximate the theoretical variability of the satellite data for a surface that corresponds to the representative surface area of the in-situ sensors. For example, you could neutralize the scale effect that makes the comparison between the two measurement techniques more difficult. In the end, this may answer the question whether the variability is due to the scale effect or due to other factors that should be considered.

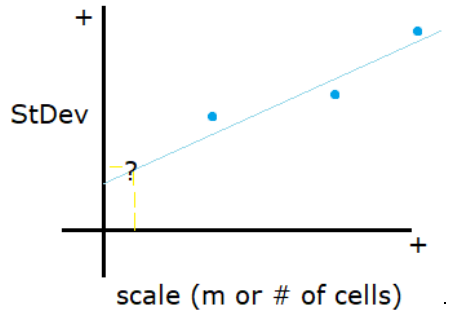

Figure 5.2 Simplified example of the proposed downscaling method to approximate the variability at a smaller spatial scale.

6
Conclusions

The research showed that as of begin 2020 there is only a limited number of operational (remote sensing) data products that map soil moisture content across the Netherlands. The available products that were found during the research are OWASIS (by HydroLogic) and the VanderSat soil moisture product. OWASIS maps at 250m resolution and VanderSat maps at 100m resolution. Both products are updated on a daily basis where possible.

The analyses that were done to assess the reliability and accuracy of the available products showed that the Pearson correlation with in-situ measurements at a depth of 5 cm (WSAM) to 20 cm (WSBD) below surface level was better for the VanderSat (L-band) product than for OWASIS: OWASIS showed a weak correlation to in-situ measurements, with Pearson correlations of R=0.29 (*single cell site average*), 0.31 (*3x3-grid*), 0.18 (*catchment scale*). These low correlations are likely explained by the fact that OWASIS models the soil moisture content in the rootzone rather than the full unsaturated zone, in addition the extent of the modelled rootzone can vary over time and space. The product does not report the modeled depth of the rootzone, rendering the data unusable for inundation risk assessment. The VanderSat product showed a moderate to strong correlation with in-situ measurements: R=0.66 (*single cell site average*) and R=0.82 (*catchment scale*). The mean absolute error for VanderSat compared to in-situ measurements was 0.068 [m^3/m^3] (*single cell*) and 0.031 [m^3/m^3] (at *catchment scale*). The spatial and temporal variability in soil moisture content among individual sites was much higher in-situ compared to the VanderSat product; this might partly be explained by some (possibly) erroneous in-situ measurements that showed uncommon soil moisture values for sandy soils of <0.05 and >0.4 [m^3/m^3], but it is assumed more likely that the lack of variability is an inherent property of the VanderSat product. This is assumed because literature shows that soil moisture is generally highly variable. This means that the actual variability is much higher than what VanderSat shows.

It was concluded that the number of in-situ sites was too low to find significant trends that could explain differences in correlation between sites, i.e. relating the correlations to specific soil type, groundwater levels or land-use types.

The basic rainfall-runoff analysis showed that for precipitation events in the study area the groundwater depth generally has more influence on the discharge than the soil moisture content. This was shown by the fact that there was a clear gradient from low to high discharge when transitioning from (relatively) deep to medium to shallow groundwater levels; while for the soil moisture content the transition from medium to wet conditions showed more of a mixed pattern, i.e. some wet conditions showed medium discharges and some medium soil moisture conditions showed high discharge. Though, in certain cases the importance of groundwater levels on discharge generation is exceeded (or overruled) by the soil moisture conditions, as was shown by a small number of events in which the groundwater level was relatively close to the surface, while discharge remained low due to dry soil moisture conditions.

Thus, it is likely that soil moisture products that are based on remote sensing data are currently an unfeasible option to improve the assessment of near-future inundation risk for the province of Noord-Brabant, the Netherlands, because the available products are either unreliable or too smooth to provide accurate soil moisture content estimates at cell scale (100 - 250 m resolution). The VanderSat product has some potential to be used at catchment scale (approx. 100 km^2 in the research), but it depends on the application whether this is sufficient for operational use. In addition, it was shown that soil moisture conditions are generally less important in (high) runoff generation than the level of the groundwater. Thus, for general near-future inundation risk assessment it would be advisable to focus on other options than remote sensing soil moisture content. Optionally, further research could be done to assess what factors determine conditions were soil moisture content is more important than (for example) groundwater, but it is only advisable to do so after the quality of remote sensing soil moisture products would improve.

Bibliography

Bastiaanssen, W. G., Menenti, M., Feddes, R. A., & Holtslag, A. A. M. (1998). A remote sensing surface energy balance algorithm for land (SEBAL). 1. Formulation. *Journal of hydrology*, *212*, 198-212.

Benninga, H. F., Carranza, C. D., Pezij, M., Van der Ploeg, M. J., Augustijn, D. C. M., & Van der Velde, R. (2018). Regional soil moisture monitoring network in the Raam catchment in the Netherlands.

Benninga, H. J. F., van der Velde, R., & Su, Z. (2019). Impacts of Radiometric Uncertainty and Weather-Related Surface Conditions on Soil Moisture Retrievals with Sentinel-1. *Remote sensing*, *11*(17), 2025.

Bilskie, J. (2001). Soil water status: content and potential [PDF]. *Campbell Scientific, Inc.* Retrieved April 10, 2020, from http://s.campbellsci.com/documents/ca/technical-papers/soilh20c.pdf.

de Jeu, R. A., Holmes, T. R., Parinussa, R. M., & Owe, M. (2014). A spatially coherent global soil moisture product with improved temporal resolution. *Journal of Hydrology, 516, 284-296*.

de Jeu, R. A. & de Nijs, A. (2017). Evaluatie van hoge resolutie satelliet bodemvochtproducten met behulp van grondwaterstandmetingen. *Stromingen: vakblad voor hydrologen. 23(2017)2. Pp. 23-34*. Retrieved April 8, 2020, from https://edepot.wur.nl/455412.

Dobson, M. C., Ulaby, F. T., Hallikainen, M. T., & El-Rayes, M. A. (1985). Microwave dielectric behavior of wet soil-Part II: Dielectric mixing models. *IEEE Transactions on Geoscience and Remote Sensing*, (1), 35-46.

Entekhabi, D., Njoku, E. G., O'Neill, P. E., Kellogg, K. H., Crow, W. T., Edelstein, W. N., ... & Kimball, J. (2010). The soil moisture active passive (SMAP) mission. *Proceedings of the IEEE*, *98*(5), 704-716.

Evans, R. O., & Sneed, R. E. (1991). Measuring soil water for irrigation scheduling: Monitoring methods and devices. *AG-North Carolina Agricultural Extension Service, North Carolina State University (USA)*. Retrieved April 1, 2020 from https://content.ces.ncsu.edu/measuring-soil-water-for-irrigation-scheduling

Feddes, R. A., Van Dam, J. C., & Witte, J. P. M. (2003). *Soil Physics and Agrohydrology*. Wageningen Universiteit.

Franz, T. E., Zreda, M., Rosolem, R., & Ferre, T. P. A. (2013). A universal calibration function for determination of soil moisture with cosmic-ray neutrons. *Hydrology and Earth System Sciences*, *17*(2), 453.

Hendriks, M. (2010). *Introduction to Physical Hydrology* (1st ed.). Oxford, United Kingdom: Oxford University Press.

Hydrologic. (2012, February 13). Neerslaginformatie op basis van Nederlandse en buitenlandse radars nu beschikbaar [white paper]. Retrieved April 14, 2020, from https://www.hydrologic.nl/files/Internationaal-RadarComposiet-HydroLogic.pdf.

Hydrologic. (2018, May 15). Actuele vullingsgraad bodem [presentation slides]. Retrieved March 31, 2020, from https://edepot.wur.nl/451413.

Hydrologic. (2019). OWASIS: essentiële informatie voor het waterbeheer nu beschikbaar. Retrieved March 12, 2020 from https://www.hydrologic.nl/owasis-essentiele-informatie-voor-het-waterbeheer/.

Jaiswal, R. K., Ali, S., & Bharti, B. (2020). Comparative evaluation of conceptual and physical rainfall–runoff models. *Applied Water Science*, *10*(1), 1-14.

Knotters, M., Walvoort, D. J. J., Brouwer, F., Stuyt, L. C. P. M., & Okx, J. P. (2018). Landsdekkende, actuele informatie over grondwatertrappen digitaal beschikbaar. *H2O online*.

Kokkonen, T. S., & Jakeman, A. J. (2001). A comparison of metric and conceptual approaches in rainfall-runoff modeling and its implications. *Water Resources Research*, *37*(9), 2345-2352.

Lillesand, T. M., Kiefer, R. W., & Chipman, J. W. (2000). Remote sensing and image interpretation. John Willey & Sons. *New York*, *724*.

Lopez-Baeza, E. (August, 2012). Physical Principles of Passive Microwave Radiometry. Soil Moisture. [Powerpoint Slides]. Retrieved April 7, 2020, from https://earth.esa.int/documents/973910/1002056/EL1.pdf/5912c3ab-a36f-4d76-900a-9c6ed4b5cc36.

Ma, Y., Wu, H., Wang, L., Huang, B., Ranjan, R., Zomaya, A., & Jie, W. (2015). Remote sensing big data computing: Challenges and opportunities. *Future Generation Computer Systems*, *51*, 47-60.

Mahmood, R., & Hubbard, K. G. (2007). Relationship between soil moisture of near surface and multiple depths of the root zone under heterogeneous land uses and varying hydroclimatic conditions. *Hydrological Processes: An International Journal*, *21*(25), 3449-3462.

METER Group. (n.d.). Soil moisture sensors—How they work. Why some are not research-grade. Retrieved April 17, 2020, from https://www.metergroup.com/environment/articles/tdr-fdr-capacitance-compared/.

Moradkhani, H. (2008). Hydrologic remote sensing and land surface data assimilation. *Sensors*, *8*(5), 2986-3004.

Mulder, M. (2018). Monitoring land restoration projects of Justdiggit in Kenya, using downscaled passive microwave remote sensing products of VanderSat [Master Thesis]. Retrieved April 8, 2020 from https://repository.tudelft.nl/islandora/object/uuid:86a24122-e3b5-4cc7-b580-f70fdecb78f8

Njoku, E. G., & Kong, J. A. (1977). Theory for passive microwave remote sensing of near-surface soil moisture. *Journal of Geophysical Research*, *82*(20), 3108-3118.

Owe, M., de Jeu, R., & Walker, J. (2001). A methodology for surface soil moisture and vegetation optical depth retrieval using the microwave polarization difference index. *IEEE Transactions on Geoscience and Remote Sensing, 39(8), 1643-1654*.

Pelgrum, H., Miltenburg, I., Cheema, M., Klaasse, A., & Bastiaanssen, W. (2010, September). ETLook a novel continental evapotranspiration algorithm. In *Remote Sensing and Hydrology Symposium, Jackson Hole, Wyoming, USA*.

Petropoulos, G. P., Ireland, G., & Barrett, B. (2015). Surface soil moisture retrievals from remote sensing: Current status, products & future trends. *Physics and Chemistry of the Earth, Parts A/B/C*, *83*, 36-56.

Reichle, R. H. (2008). Data assimilation methods in the Earth sciences. *Advances in water resources*, *31*(11), 1411-1418.

Ritzema, H. P., Heuvelink, G. B. M., Heinen, M., Bogaart, P. W., van der Bolt, F. J. E., Hack-ten Broeke, M. J. D., ... & Vroon, H. R. J. (2012). *Meten en interpreteren van grondwaterstanden: analyse van methodieken en nauwkeurigheid* (No. 2345). Alterra.

Sabins, F. (1997). Remote Sensing: Principles and Interpretation. *WH Freeman and Company.*

Sadeghi, M., Babaeian, E., Ebtehaj, A. M., Jones, S. B., & Tuller, M. (2018). Remote Sensing of Environmental Variables and Fluxes. *Handbook of Environmental Engineering*. pp. 249–302. doi:10.1002/9781119304418.ch9.

Santanello Jr, J. A., & Carlson, T. N. (2001). Mesoscale simulation of rapid soil drying and its implications for predicting daytime temperature. *Journal of Hydrometeorology*, *2*(1), 71-88.

Schmugge, T.J. (1985). Remote sensing of soil moisture. In Anderson, M. And Burt, T., editors, Hydrological Forecasting. John Wiley, New York.

STOWA. (2016). *Verkenning remote sensing producten voor het waterbeheer*.

Toorn, L., Klutman, W. A. J., Hanhart-van den Brink, M., Heijkers, J., van Bakel, J., Bastiaanssen, M., ... & Veldhuizen, A. A. (2016). Nowcasten actuele vullingsgraad bodem (met behulp van een model en remote sensing data) *(No. 2016-20). Stowa*.

TU Delft. (n.d.). Data Assimilation. Retrieved April 20, 2020, from https://www.tudelft.nl/en/ceg/about-faculty/departments/watermanagement/research/chairs/water-resources/water-resources-management/research/tools/data-assimilation/.

van Dam, J. C., Groenendijk, P., Hendriks, R. F., & Kroes, J. G. (2008). Advances of modeling water flow in variably saturated soils with SWAP. *Vadose Zone Journal*, *7*(2), 640-653.

van den Brink, M., Heijkers, J., van Leeuwen, H. (2019). OWASIS: Actuele bodemvocht-informatie helpt de operationeel waterbeheerder. *Water Matters, september 2019, pp. 32-35.*

van der Schalie, R., de Jeu, R. A., Kerr, Y. H., Wigneron, J. P., Rodríguez-Fernández, N. J., Al-Yaari, A., ... & Drusch, M. (2017). The merging of radiative transfer based surface soil moisture data from SMOS and AMSR-E. *Remote Sensing of Environment*, *189*, 180-193.

van der Velde, R., Colliander, A., Pezij, M., Benninga, H.-J. F., Bindlish, R., Chan, S. K., Jackson, T. J., Hendriks, D. M. D., Augustijn, D. C. M., and Su, Z. (2019). Validation of SMAP L2 passive-only soil moisture products using *in situ* measurements collected in Twente, The Netherlands, *Hydrol. Earth Syst. Sci. Discuss.*, https://doi.org/10.5194/hess-2019-471, in review, 2019.

VanderSat. (n.d.) VanderSat Frequently Asked Questions (FAQ). Retrieved April 1, 2020 from http://docs.vandersat.com/VanderSat_FAQ.html.

Van Walsum, P. E. V., & Veldhuizen, A. A. (2011). *MetaSWAP_V7_2_0. Rapportage van activiteiten ten behoeve van certificering met Status A* (No. 276). WUR.

Wang, L., & Qu, J. J. (2007). NMDI: A normalized multi-band drought index for monitoring soil and vegetation moisture with satellite remote sensing. *Geophysical Research Letters*, *34*(20).

Wang, L., & Qu, J. J. (2009). Satellite remote sensing applications for surface soil moisture monitoring: A review. *Frontiers of Earth Science in China*, *3*(2), 237-247.

Western, A. W., & Blöschl, G. (1999). On the spatial scaling of soil moisture. *Journal of hydrology*, *217*(3-4), 203-224.

Wosten, J. H. M., de Vries, F., Hoogland, T., Massop, H. T. L., Veldhuizen, A. A., Vroon, H. R. J., ... & Bolman, A. (2013). BOFEK2012, de nieuwe bodemfysische schematisatie van Nederland. *(No. 2387). Alterra*.

Wu, Q., Liu, H., Wang, L., & Deng, C. (2016). Evaluation of AMSR2 soil moisture products over the contiguous United States using in situ data from the International Soil Moisture Network. *International journal of applied earth observation and geoinformation*, *45*, 187-199.

Ye, N., Walker, J. P., Rüdiger, C., Ryu, D., & Gurney, R. J. (2019). Impact of Urban Cover Fraction on SMOS and SMAP Surface Soil Moisture Retrieval Accuracy. *IEEE Journal of Selected Topics in Applied Earth Observations and Remote Sensing*, *12*(9), 3338-3350.

Zhuo, L., & Han, D. (2016). The relevance of soil moisture by remote sensing and hydrological modelling. *Procedia Engineering*, *154*, 1368-1375.

Zreda, M., Shuttleworth, W. J., Zeng, X., Zweck, C., Desilets, D., Franz, T., & Rosolem, R. (2012). COSMOS: the cosmic-ray soil moisture observing system. *Hydrology & Earth System Sciences*, *16*(11):4079.

Zwieback, S., Paulik, C., & Wagner, W. (2015). Frozen soil detection based on advanced scatterometer observations and air temperature data as part of soil moisture retrieval. *Remote Sensing*, *7*(3), 3206-3231.

Appendix A

Soil moisture remote sensing products available for the Netherlands

Table B1 End-user products for soil moisture monitoring in the Netherlands, as of Q2 2020.

Product	Available data	Outputs	Spatial resolution [m]	Spatial extent	Temporal resolution	Sensing depth [cm]	Rootzone options [cm]	Notes
OWASIS (HydroLogic)	Jan 2016 - now (+2-day forecast)	Soil moisture (mm), Available soil storage (mm), Groundwater level (mNAP)	250 m	Netherlands	Daily	-	Location specific	Based on water balance model (MODFLOW-MetaSWAP), using precipitation (ground radar) and actual evapotranspiration (satellite).
VanderSat soil moisutre	June 2002 - now	Soil moisture (m^3/m^3)	100 m	Global	Daily	0-5 cm	10, 20, 40 cm	Based on passive microwave radiometer satellites (e.g. AMSR-2, SMAP).

Table B2 Satellite products for soil moisture monitoring in the Netherlands, as of Q2 2020.

Mission / Satellite / Sensor	Launch / operational time	Sensor type	Spatial resolution [m]	Temporal resolution [days]	Notes
Sentinel-1 (S1-A & S1-B) (ESA)	S1-A: April 2014 - now S1-B: April 2016 - now	C-band radar (SAR)	5, 20, 100 m (mode-dependent)	10 (S1-A or B) 5 (S1-A+B)	Available data products: level-0, level-1. The ESA Toolbox allows the user to derive level-2 products
Radarsat-2	2012 - 2016 (25m) 2015 - now (5m)	C-band radar	24 m	2.25 (mode-dependent)	Commercial sensor. Images of the Netherlands are available free of charge through the Satellietdataportaal.
SMAP (NASA)	2015 - now	L-band radar & microwave radiometer	10 km (active), 40 km (passive)	2-3	Specially developed for measuring soil moisture. Unfortunately, radar is no longer operational. Only radiometer still works. Available data products: level-1 (radiometer data) Level-2 to level-4 (soil moisture data)
SMOS (ESA)	2009 - now	L-band microwave radiometer	30 km	2-3	Specially developed for measuring soil moisture. Available data products via ESA: Level-1 brightness temperature Level-2 (soil moisture data)
ASCAT (EUMETSAT) onboard Metop-A, B and C	2006 - 2020	C-band scatterometer (radar)	25/50 km	1-2 (Metop-A or Metop-B), <1 (Metop-A+B)	ASCAT has been specifically developed for measuring wind above the sea. However, the derived soil moisture products are not inferior to SMOS and SMAP. Available Products: ASCAT-SSM (soil moisture top layer) ASCAT-SWI (soil moisture root zone)
AMSR2 (JAXA)	2012 - now	Microwave radiometer	10/25 km	1-2	Wide range of data and products available, ranging from level 1 to 3.

An overview of satellite products of the Netherlands (not limited to soil moisture applications) that are available free of charge for Dutch users, can be found at: https://www.spaceoffice.nl/nl/satellietdataportaal/beschikbare-data/ (in Dutch).

Appendix B

Microwave remote sensing bands and surface roughness classification

Table B.1 Radar band designations (Lillesand *et al*., 2000, p.659).

Band designation	**Wavelength λ (cm)**	**Frequency (GHz)**
Ka	0.75 – 1.1	40 – 26.5
K	1.1 – 1.67	26.5 – 18
Ku	1.67 – 2.4	18 – 12.5
X	2.4 – 3.75	12.5 – 8
C	3.75 – 7.5	8 – 4
S	7.5 – 15	4 – 2
L	15 – 30	2 – 1
P	30 – 100	1 – 0.3

Table B.2 Definition of Synthetic Aperture Radar Roughness.
Categories for three local incident angles, based on the modified Rayleigh criterion (adapted from Sabins, 1997).

Roughness Category	Root-Mean-Squared Surface Height Variation (cm)		
	Ka Band (λ = 0.86 cm)	X Band (λ = 3.2 cm)	L Band (λ = 23.5 cm)
(*a*) Local indidence angle of 20°			
Smooth	<0.04	<0.14	<1.00
Intermediate	0.04-0.21	0.14-0.77	1.00-5.68
Rough	>0.21	>0.77	>5.68
(*b*) Local incidence angle of 45°			
Smooth	<0.05	<0.18	<1.33
Intermediate	0.05-0.28	0.18-1.03	1.33-7.55
Rough	>0.28	>1.03	>7.55
(*c*) Local incidence angle of 70°			
Smooth	<0.10	<0.37	<2.75
Intermediate	0.10-0.57	0.37-2.13	2.75-15.6
Rough	>0.57	>2.13	>15.6

Appendix C

Correlation by soil type, groundwater levels & land-use type

C1 Correlation per soil type (BOFEK2012)

BOFEK2012 is a national map of soil type classifications in the Netherlands (Wosten *et al.,* 2013). Table C.1 shows the BOFEK2012 unit (soil type) at each soil moisture site. Tables C.2a and C.2b show the BOFEK unit and corresponding Pearson correlations for the OWASIS *3x3-grid* and VanderSat *single cell* data, respectively.

Table C.1 BOFEK2012 soil type per site.

ID	BOFEK2012	Description (Dutch)
WSBD_Bavel	310	Zwak lemige zandgronden met een matig dik cultuurdek
WSBD_Rijsbergen	304	Zwak lemige (podzol-)gronden
WSAM_Bult	205	Zanddek op moerige tussenlaag op zandondergrond
WSAM_Raam_01	305	Zwak lemige zandgronden met grof zand in de ondergrond
WSAM_Raam_02	305	Zwak lemige zandgronden met grof zand in de ondergrond
WSAM_Raam_03	304	Zwak lemige (podzol-)gronden
WSAM_Raam_04	305	Zwak lemige zandgronden met grof zand in de ondergrond
WSAM_Raam_05	311	Zwak lemige zandgronden met een dik cultuurdek (enkeerdgronden)
WSAM_Raam_06	409	Lichte zavel op zand (fluviatiel)
WSAM_Raam_07	317	Lemige zandgronden met een dik cultuurdek (enkeerdgronden)
WSAM_Raam_08	304	Zwak lemige (podzol-)gronden
WSAM_Raam_09	304	Zwak lemige (podzol-)gronden
WSAM_Raam_10	304	Zwak lemige (podzol-)gronden
WSAM_Raam_11	304	Zwak lemige (podzol-)gronden
WSAM_Raam_12	304	Zwak lemige (podzol-)gronden
WSAM_Raam_13	309	Zwak lemige (beekeerd-)gronden deels met grof zand in de ondergrond
WSAM_Raam_14	312	Lemige (podzol-)gronden
WSAM_Raam_15	311	Zwak lemige zandgronden met een dik cultuurdek (enkeerdgronden)

Table C.2a BOFEK2012 soil types and Pearson correlation (OWASIS *3x3-grid*) by number of sites. n=15 (18). *Brackets indicate sites that were only present in the OWASIS dataset.*

	205	304	305	309	310	311	312	317	409
≤ 0.29	(1)	4	2	1		1	1	1	
0.3 – 0.39		1							
0.4 – 0.49									
0.5 – 0.59		1				1			
0.6 – 0.69		(1)			(1)				1
0.7 – 0.80			1						

Table C.2b BOFEK2012 soil types and Pearson correlation (VanderSat *single cell*) by number of sites. n=15.

	205	304	305	309	310	311	312	317	409
0.3 – 0.39									
0.4 – 0.49		1							
0.5 – 0.59		3		1					1
0.6 – 0.69			1						
0.7 – 0.80		2	2			2	1	1	

C2 Correlation per groundwater level classification (*grondwatertrappen)*

In the Netherlands, groundwater depths are classified as '*grondwatertrappen*', which give an indication of the absolute groundwater level and its fluctuation. The classes are defined on the basis of the average highest groundwater level (abbreviated as GHG) and average lowest groundwater level (GLG) (Table C.3). The groundwater classes are indicated with a Roman numeral (I – VIII), with a higher number indicating that the groundwater is predominantly deeper below surface level. Table C.4 shows the groundwater level classification at each soil moisture site.

For the groundwater classifications a different dataset was used for WSBD compared to WSAM. The dataset for the WSBD area was created in 2010 and that of WSAM was created in 2005. It is expected that the groundwater classifications have not changed significantly from 2005 to 2010, because these classifications are generally calculated from long-term groundwater level measurements over a period of 30 years (Ritzema *et al*, 2012).

Table C.3 Groundwater level classifications (*Grondwatertrappen*). (Simplified from: Knotters, 2018).

Grondwatertrap	GHG (cm-surface)	GLG (cm-surface)
I	< 20	< 50
II	25 – 50	50 – 80
III	< 40	80 – 120
IV	> 40	80 – 120
V	< 40	> 120
VI	40 – 80	> 120
VII	> 80	-
VIII	> 140	-

Table C.4 Groundwater level classification (*grondwatertrap)* at the soil moisture sites.

ID	Grondwatertrap
WSBD_Bavel	VII
WSBD_Rijsbergen	VI
WSAM_Bult	VI
WSAM_Raam_01	IV
WSAM_Raam_02	VII
WSAM_Raam_03	III
WSAM_Raam_04	VI
WSAM_Raam_05	VIII
WSAM_Raam_06	V
WSAM_Raam_07	VII
WSAM_Raam_08	VII
WSAM_Raam_09	VI
WSAM_Raam_10	VI
WSAM_Raam_11	VI
WSAM_Raam_12	VI
WSAM_Raam_13	VI
WSAM_Raam_14	VII
WSAM_Raam_15	VI

Table C.5a *Grondwatertrap* and Pearson correlation (OWASIS *3x3*) by number of sites. n=15 (18).

	III	IV	V	VI	VII	VIII
≤ 0.29	1	1		5	3	
0.3 – 0.39						
0.4 – 0.49				1		
0.5 – 0.59				(1)	1	1
0.6 – 0.69			1			
0.7 – 0.80				1 (2)	(1)	

Table C.5b *Grondwatertrap* and Pearson correlation (VanderSat *single cell*) by number of sites. n=15.

	III	IV	V	VI	VII	VIII
0.3 – 0.39						
0.4 – 0.49				1		
0.5 – 0.59	1		1	3		
0.6 – 0.69		1				
0.7 – 0.80				3	4	1

C3 Correlation per land-use type

For the land-use classification only two classes (agricultural and grassland) were included. This two-class classification was done for simplicity, but even differentiating between the two turned out difficult as it was based on only one document from WSAM, complemented with optical satellite imagery. In some cases, the main field was agricultural, but the sensor was placed in a grassland strip at the edge of the field. The results showed that here was no difference in obtained correlation between agricultural field and grassland (Table C.6), but due to the fact that the classification is uncertain, the results are too unreliable to be used for firm conclusions.

Table C.6 Land-use type and Pearson correlations per soil moisture site. *Land-use is classified based on RGB satellite imagery (2016-2019) and documentation from Waterschap Aa en Maas (2016). In uncertain cases both classes are used.*

	Agricultural field	**Grassland**	**OWASIS *3x3-grid* Pearson (R)**	**VanderSat *single cell* Pearson (R)**
WSAM_Raam_01		x	0.19	0.61
WSAM_Raam_02	x	x	-0.25	0.83
WSAM_Raam_03		x	0.20	0.59
WSAM_Raam_04		x	0.78	0.80
WSAM_Raam_05	x		0.54	0.72
WSAM_Raam_06		x	0.64	0.53
WSAM_Raam_07	x		0.09	0.79
WSAM_Raam_08	x	x	0.51	0.78
WSAM_Raam_09	x		0.46	0.45
WSAM_Raam_10		x	-0.04	0.58
WSAM_Raam_11	x		0.21	0.74
WSAM_Raam_1	x	x	-0.05	0.56
WSAM_Raam_13	x		-0.11	0.54
WSAM_Raam_14		x	-0.11	0.73
WSAM_Raam_15		x	0.00	0.70

Table C.7 Averaged Pearson correlation (R) per land-use type.

	Agricultural field	**Grassland**
OWASIS *3x3 grid*	0.18	0.19
VanderSat *single cell*	0.68	0.67